Global and Planetary Change xxx (xxxx) 104158

Contents lists available at ScienceDirect

Global and Planetary Change

journal homepage: www.elsevier.com/locate/gloplacha

Driving processes of relative sea-level change in the Adriatic during the past two millennia: From local tectonic movements in the Dubrovnik archipelago (Jakljan and Šipan islands) to global mean sea level contributions (Central Mediterranean)

Sanja Faivre [a, *], Tatjana Bakran-Petricioli [b], David Kaniewski [c, d], Nick Marriner [e], Bruno Tomljenović [f], Marin Sečanj [g], Davor Horvatić [h], Jadranka Barešić [i], Christophe Morhange [j, l], Russell N. Drysdale [k]

[a] University of Zagreb, Faculty of Science, Department of Geography, Marulićev trg 19/II, Zagreb 10 000, Croatia
[b] University of Zagreb, Faculty of Science, Department of Biology, Rooseveltov trg 6, Zagreb 10 000, Croatia
[c] TRACES, UMR 5608 CNRS, Université Toulouse Jean Jaurès, Maison de la Recherche, 5 allées A. Machado, Toulouse Cedex 9 31058, France
[d] Université Paul Sabatier Toulouse 3, 118 Route de Narbonne, Toulouse Cedex 9 31062, France
[e] CNRS, ThéMA, Université de Franche-Comté, UMR 6049, MSHE Ledoux, 32 rue Mégevand, Besançon Cedex 25030, France
[f] University of Zagreb, Faculty of Mining, Geology and Petroleum Engineering, Pierottijeva 6, Zagreb 10000, Croatia
[g] University of Zagreb, Faculty of Science, Department of Geophysics, Horvatovac 95, Zagreb 10 000, Croatia
[h] University of Zagreb, Faculty of Science, Department of Physics, Bijenička 32, Zagreb 10 000, Croatia
[i] Ruđer Bošković Institute, Radiocarbon Laboratory, Bijenička 54, Zagreb 10 000, Croatia
[j] Aix-Marseille Université, CEREGE UMR 7330, Institut Universitaire de France, Europôle de l'Arbois, BP 80, Aix-en-Provence Cedex 04 13545, France
[k] University of Melbourne, School of Geography, Earth and Atmospheric Sciences, Melbourne, Parkville, VIC 3010, Australia
[l] EPHE-Section des Sciences Historiques et Philologiques, AOROC, UMR 8546, CNRS/PSL, France

ARTICLE INFO

Editor: Liviu Matenco

Keywords:
Lithophyllum rim
Global mean sea-level curve
Sea surface temperature
Coseismic uplift
Solar cycles
Salinity oscillations

ABSTRACT

New high-resolution relative sea-level (RSL) proxy data obtained from *Lithophyllum* rims in the Adriatic allow us to distinguish major local, regional and global RSL driving processes during the past two millennia. RSL change on the Elafiti islands in the Dubrovnik archipelago (Southern Adriatic) has been significantly affected by local tectonic contributions, which vary spatially and increase southeastwards from Jakljan to Grebeni. Consequently, the RSL change on northwestward islands, Jakljan and Šipan, is still dominantly driven by linear regional glacio-isostatic adjustment (GIA) processes estimated at ~0.34 mm/yr. However, GIA effects are occasionally cancelled out by local, non-linear coseismic uplifts of small magnitude and by variations in the global mean sea level (GMSL). Thus the rapid fall in GMSL of 0.26 mm/yr offset the GIA effects between approximately ~1000–1250 cal AD, resulting in temporal hiatuses in algal rim formation. After ~1800 cal AD, GIA rates were significantly amplified by GMSL rise, which exceed 0.9 mm/yr at Jakljan and Šipan and goes up to 1.4 mm/yr at Koločep and Grebeni, confirming the acceleration of RSL rise over the past two hundred years.

The new GMSL records from the northern and southern Adriatic, allow us to reconstruct the first high-resolution GMSL curve for the Adriatic. We show that GMSL variability is in-phase with solar activity during the last two millennia, acting on cycles of ~350, 220 and 100-yrs. We also show that increased GMSL fall, which stopped the formation of algal rims around ~1000 and ~ 1600 cal AD, coincides with the global reduction in radiative forcing associated with the Oort and Maunder minima, with a drop in sea surface temperature (SST) and with increased salinity. Thus, our analyses revealed a consistent periodicity between the Adriatic GMSL signal, solar forcing, SST and salinity, with the most important cycle being the 350-year Great Solar Cycle.

* Corresponding author.
E-mail address: sfaivre@geog.pmf.hr (S. Faivre).

https://doi.org/10.1016/j.gloplacha.2023.104158
Received 10 March 2023; Received in revised form 17 May 2023; Accepted 23 May 2023
0921-8181/

1. Introduction

Relative sea-level (RSL) change is the sum of processes acting at local, regional and global scales. Global scale sea-level changes are driven by processes that cause changes in the volume or mass of the world ocean and result in globally uniform mean sea-level variations (Rovere et al., 2016). Regional and local-scale processes, the RSL component, relates primarily to glacial isostatic adjustment (GIA); changes due to ocean dynamics; gravitational, rotational, and deformational responses to barystatic changes (Gregory et al., 2019); sediment compaction and tectonics (Walker et al., 2021). These processes vary spatially and cause variations in rates and magnitudes of RSL change between sites (Stammer et al., 2013).

Differentiating and quantifying the processes that drive RSL change provide a baseline to probe three areas: link climate change to sea-level change (Kopp et al., 2016; Kemp et al., 2018; Kench et al., 2020), improve glacio-isostatic adjustment (GIA) models by providing constraints for their calibration (e.g. Lambeck et al., 2014; Kench et al., 2020), and to better understand local and regional nonlinear processes, i.e. approaching local and regional tectonics, the most variable and uncertain component of RSL change (e.g. Faivre et al., 2019a, 2021a, 2021b).

A clear distinction must be made between improvements in understanding RSL forcings during the last 30 years, based on new techniques related to high-precision satellite measurements and new Argo float-derived estimates (e.g. Rietbroek et al., 2016; Cazenave et al., 2018), and the preinstrumental period (e.g. Kopp et al., 2016; Kemp et al., 2018; Kench et al., 2020; Walker et al., 2021). Studies of preinstrumental timescales are spatially discontinuous and limited to time slices. Therefore, to improve understanding of the magnitudes, rates, and driving processes of RSL change at all scales (local, regional and global) and in different geomorphological and geological contexts, there is a need for diverse kinds of RSL proxy records (e.g. Morhange and Marriner, 2015; Khan et al., 2019; Dean et al., 2019; Onac et al., 2022) which can provide robust high-resolution RSL reconstructions.

Salt-marsh sediments are very good archives for reconstructions of RSL changes on clastic coasts (e.g. Gehrels et al., 2005; Kemp et al., 2018) providing high-resolution records spanning the past 3000 years, particularly for the US and Canadian (North American) Atlantic seaboard (e.g. Kemp et al., 2015, 2018).

Fixed biological markers are considered one of the most reliable RSL indicators on rocky coasts. They form at a well-defined elevation within the tidal frame. Likewise, bioconstructions formed by coralline algae or vermetid gastropods are particularly important indicators outside the tropical coral reef belt, particularly in the Mediterranean (e.g. Laborel et al., 1994; Morhange, 1994; Silenzi et al., 2004; Sisma-Ventura et al., 2009).

Under favourable conditions, coralline algae *Lithophyllum byssoides* (Lamarck) Foslie may build up reef-like bioconstructions, called *Lithophyllum* rims, just above the biological mean sea-level (MSL) (Pérès and Picard, 1964; Laborel and Laborel-Deguen, 1994), which may provide robust records of RSL change (Morhange et al., 2001; Faivre et al., 2019a, 2021a, 2021b). When submerged or uplifted, remains of *Lithophyllum rims* may be preserved and can be used in reconstructions of coastal evolution (Laborel et al., 1994; Ferranti et al., 2006; Spampinato et al., 2014; Sechi et al., 2018, 2020; Faivre et al., 2019a, 2021a, 2021b). Due to the narrow altitudinal band of L. *byssoides* habitats (Stewart and Morhange, 2009; Faivre et al., 2021a, 2021b) and the fact that biological formations are well suited to radiocarbon dating, algal rims constitute excellent archives of RSL change on rocky coasts.

The potential of *Lithophyllum rims* as a RSL marker was recognised several decades ago in the Western Mediterranean (Laborel et al., 1983; Morhange, 1994). However, the determination of marine radiocarbon reservoir effects (Faivre et al., 2019b) has increased the chronological resolution of the rims and allowed them to be used as high-resolution RSL markers (Faivre et al., 2019a, 2021a, 2021b). The algal rims can also be used as precise indicators of palaeoseismic events and tectonic uplift (Faivre et al., 2021a, 2021b). Furthermore, *L. byssoides* stable isotope composition can provide insights into the palaeoclimate trends (Faivre et al., 2019a), which are important for the development of regional climate models, and future regional predictions of RSL change.

Along the eastern Adriatic coast, the number of reconstructions of RSL change (e.g. Fouache et al., 2000; Faivre et al., 2011, 2019a, 2021a, 2021b; Marriner et al., 2014; Faivre and Butorac, 2018; Shaw et al., 2018; Brunović et al., 2020; Razum et al., 2020; Kaniewski et al., 2021; Ilijanić et al., 2022) and palaeoclimate reconstructions (Lončar et al., 2017, 2019, 2022; Surić, 2018; Kaniewski et al., 2018, 2022) are constantly increasing. However, a clear differentiation between regional, local and global driving processes is still challenging.

The eastern Adriatic coast is considered to be a tectonically active area (Kuk et al., 2000; Faivre and Fouache, 2003; Prelogović et al., 2004; Korbar et al., 2009; Surić et al., 2014; Marriner et al., 2014; Faivre and Butorac, 2018; Faivre et al., 2019a, 2019b). Its northern part provides evidence of subsidence (Faivre et al., 2019a; Kaniewski et al., 2021), while those in its central and southern parts attest to Quaternary uplift (Babić et al., 2012; Korbar et al., 2009; Faivre et al., 2021a, 2021b; Šolaja et al., 2022).

The Southern Adriatic is one of the major seismogenic areas of the Central Mediterranean region, characterized by the strongest historically known and instrumentally recorded earthquakes in Croatia and Montenegro (Herak et al., 1996; Benetatos and Kiratzi, 2006; Govorčin et al., 2020; Schmitz et al., 2020). Recently in this area, Faivre et al. (2021a, 2021b) reconstructed the RSL changes of the Elafiti islands in the Dubrovnik archipelago, which are attributed to the Holocene seismotectonic activity (Fig. 1). Here, the most important seismic event is the well-known 1667 Dubrovnik earthquake that resulted in c. 0.40–0.55 ± 0.10 m of coseismic uplift. This event, together with previous and recently recorded events, is generally attributed to the Pelješac – Dubrovnik fault zone composed of NE-dipping thrusts and reverse faults striking parallel to the coastline and to the Elafiti islands.

To further improve our understanding of RSL changes in the Southern Adriatic during the past two millennia, and to obtain additional data from the NW part of Elafiti islands that has not been studied so far, we here quantify the magnitudes and rates of RSL changes on Jakljan and Šipan islands to probe the driving mechanisms of RSL changes. Thus, our goal is to distinguish local non-linear, e.g., coseismic movements related to neotectonics, from regional linear glacio-isostatic processes (GIA) and global-scale contributions.

The objective of this study is to determine the variability of local tectonic processes that contributed to past RSL changes, based on palaeoshoreline evidence from the Elafiti Islands. In this way, tectonically active coastal sections can be outlined and, tectonic blocks with different motions distinguished. Knowledge on neotectonics is important for future seismic hazard assessment in the Southern Adriatic area and its hinterland, which includes the UNESCO World Heritage site of Dubrovnik.

Furthermore, we also reconstruct sea surface temperatures (SST) based on the analysis of L. *byssoides* stable isotopes to identify local trends during the pre-industrial era. Using the same proxy provides a consistent baseline to probe the link between sea-level change and climate change.

Finally, to investigate the drivers of GMSL variations we construct the GMSL curve for the Adriatic based on homogeneous algal rim records from new and previously published data (Faivre et al., 2019a, 2021a) from the northern and southern Adriatic and analyse its variability in terms of solar forcing, SST and salinity.

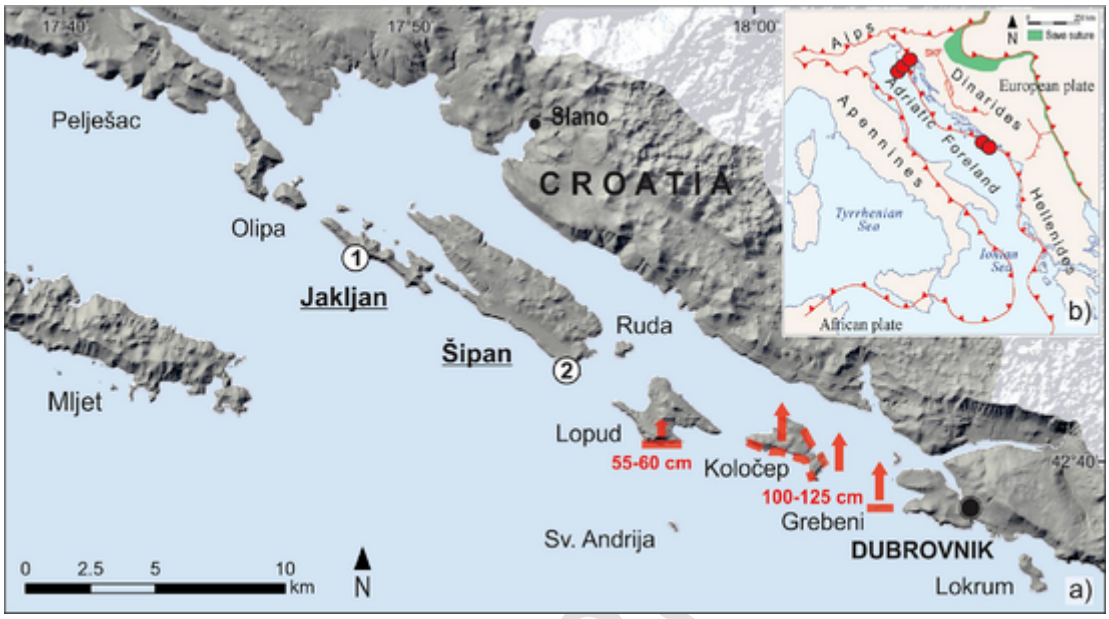

Fig. 1. Study area: a) Locations of studied algal rims at Jakljan and Šipan (Elafiti islands) in the southern Adriatic; red lines represent uplifted sectors of coast with arrows showing the cumulative uplift amplitudes in 1.6 ka; b) Locations of algal rims used for the analysis of GMSL variations on a simplified tectonic map showing the main tectonic boundaries (after Schmid et al., 2020); SKF –Split Karlovac Fault. (For interpretation of the references to colour in this figure legend, the reader is referred to the web version of this article.)

2. Study area

Elafiti islands of the Dubrovnik archipelago are located in the southern part of the eastern Adriatic coast, comprising five major islands and several islets extending in a NW-SE direction for c. 27 km from Pelješac peninsula to Dubrovnik (Fig. 1). To the NE they are separated from the mainland by NW-SE trending Koločep channel with an average width of 1.5 km. Here the seafloor in the central part of the bay is relatively flat at a depth of 50–55 m b.s.l., while at the south-eastern and northwestern ends, the seafloor is situated at depths of 30 m and 60 m b.s.l., respectively (Šolaja et al., 2022).

Our work focuses on the islands of Jakljan and Šipan, the two northernmost islands in Elafiti archipelageo separated by a narrow passage, with surface areas of 3.07 km^2 and 16.22 km^2 respectively. Šipan is the largest and most populated island of the arechipelago. It rises up to 234 m on its northern side, while Jakljan attains a height of 225 m, in its central part. The outer southwestern coast of both islands is characterized by steep cliffs. Here, the seafloor quickly falls to a depth of 50 m and then to over 100 m b.s.l. at c. 2 km distance offshore from Šipan island (Fig. 2).

The two studied locations are ~10 km apart. Together with sections and locations studied previously (Faivre et al., 2021a, 2021b), they comprise a coastal study area that extends from Jakljan to Grebeni, and covers all of Elafiti's major islands. The studied area constitutes a microtidal environment with an average amplitude of 25 cm (data from the Dubrovnik tide gauge, Hydrographic Institute of the Republic of Croatia, Split).

2.1. Tectonic setting

The study area is in the south-eastern part of the External Dinarides, the fold-thrust belt formed along the NE margin of the Adriatic microplate during the Cenozoic convergence of this microplate with the European plate (Fig. 1b; e.g. Schmid et al., 2020; van Hinsbergen et al., 2020). Tectonically, it belongs to the Dalmatian unit, the lowest tectonic unit of this fold-thrust belt, which to the SW thrusts over the Adriatic foreland and to the NE lies underneath the High Karst unit (Fig. 2; Schmid et al., 2020; Balling et al., 2021a).

Both, the Dalmatian and High Karst units mainly consist of Mesozoic shallow-marine carbonates derived from the Adriatic carbonate platform (AdCP sensu Vlahović et al., 2005), which was affected by the SW-directed thrusting in Middle – Late Eocene and Oligocene times (e.g. Balling et al., 2021a). This thrusting resulted from the Late Cretaceous–Paleocene closure of a northern branch of the Neotethys ocean (i.e., the Western Vardar ocean sensu Schmid et al., 2020), and the collision of the Adriatic and European plates along the Sava suture zone in the Internal Dinarides (Fig. 1b; Ustaszewski et al., 2010; Schmid et al., 2020).

The Middle Eocene to Oligocene SW-directed thrusting related to the main tectonic phase in the External Dinarides, resulted in the formation of Eo-Oligocene flexural foreland basin system developed along their entire length (e.g. Vlahović et al., 2012). It is mostly characterized by the deposition of the Foraminiferal Limestone of Lower and Middle Eocene age (e.g. Ćosović et al., 2018) and by prevailingly Middle Eocene to Oligocene *syn*-tectonic flysch-type and alluvial fan deposits known as the External Dinarides Flysch and the Promina Beds, respectively (e.g. Babić and Zupanič, 2008; Vlahović et al., 2012; Balling et al., 2021a).

In the south-eastern part of the External Dinarides, i.e., to the SE of the Split–Karlovac Fault (SKF in Fig. 1b), the Eo-Oligocene tectonic phase resulted in at least 127 km of shortening (Balling et al., 2021a), accommodated by a top-SW to top-S directed thrusting, reverse faulting and fault-related folding of platform carbonates and the overlying Eo-Oligocene syn-tectonic deposits (Fig. 2; see also Prtoljan et al., 2007; Balling et al., 2021a).

According to Balling et al. (2021b), the External Dinarides, together with the rest of the mountain range, experienced a post-tectonic Oligocene–Miocene (28–17 Ma) regional uplift, assumed to have been driven by the post-collisional mantle delamination of the Adriatic lithosphere. Since Miocene times, most of the External Dinarides have not experienced substantial orogen-scale shortening except for locally observed deformation mostly accommodated by NE-dipping reverse or thrust faults and by NW-striking dextral strike-slip faults that either reactivate or cut across older Eo-Oligocene tectonic contacts (van Unen et al., 2019a, 2019b).

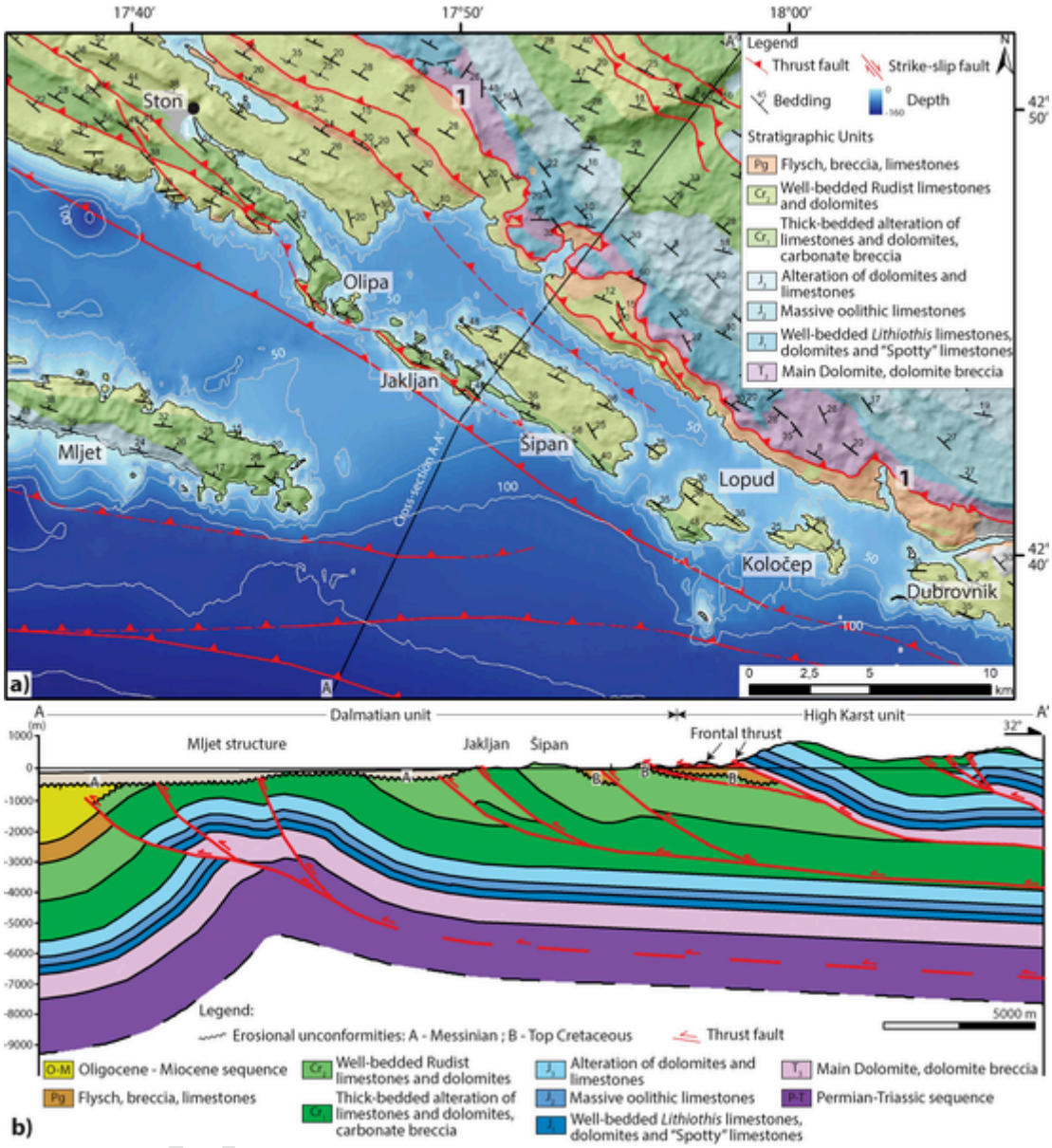

Fig. 2. Geological map of the study area (a) and simplified regional cross-section A–A' across the SW part of the High Karst and the Dalmatian unit (b). Geological map and cross-section are compiled and constructed based on the Basic Geological Map of former Yugoslavia, sheets: Trebinje (Natević and Petrović, 1967), Dubrovnik (Marković, 1971) and Ston (Raić et al., 1980), supplemented by own field measurements and by interpretation and correlation with 2D reflection seismic cross-sections.

Albeit characterized by small slip-rates ranging between 0.15 and 2.01 mm/yr (Kastelic and Carafa, 2012), these faults are considered as major seismogenic sources of historically and instrumentally recorded earthquakes in the External Dinarides (e.g. Kuk et al., 2000; Kastelic et al., 2013; Palenik et al., 2019; Govorčin et al., 2020; Schmitz et al., 2020). Their activity and seismicity are driven by ongoing convergence of the Adriatic microplate with respect to Europe at GPS-derived shortening rates of c. 3–5 mm/yr (Grenerczy et al., 2005; Bennett et al., 2008; Weber et al., 2010).

2.2. Geological setting

Like other islands in the Elaphiti archipelago, Jakljan and Šipan islands are composed of Lower and Upper Cretaceous shallow marine carbonates at the surface (Fig. 2a,b; Raić et al., 1980) originated from the Mesozoic Adriatic Carbonate platform (Vlahović et al., 2005). While Cretaceous carbonate rocks prevail in the elevated areas and along the coasts of the islands, Quaternary deposits are also present in local karst depressions and poljes in the form of sands and terra rossa (Raić et al., 1980; Kovačić et al., 2018).

On both islands Cretaceous carbonates form a concordant ~2.000 m thick sequence of alternating limestones and dolomites, starting with Hauterivian–Aptian carbonates in the central part of the Jakljan island, followed upward by Albian to Senonian carbonates exposed along the NE coast of the Šipan island. At the surface, these well-bedded carbonates moderately dip towards the NE and form a homocline (Fig. 2a), which according to the balanced cross-section A–A' shown in Fig. 2b, corresponds to the NE-dipping limb of the fault-related anticline formed in a hangingwall of the Jakljan thrust, a member of the Pelješac – Dubrovnik fault zone here comprising four major NE-dipping thrusts (Fig. 2). Presumably, they all sole out from a décollement situated near the base of the Cretaceous carbonate sequence of the Dalmatian tectonic unit (Fig. 2b) and formed by in-sequence and SW-propagating thrusting from the High Karst into the Dalmatian unit during the main

tectonic phase in the External Dinarides in Mid-Eocene – Oligocene times. The Jakljan thrust, mapped at the surface along the SW margin of this island, extends to the NW into the Pelješac peninsula and puts Lower onto Upper Cretaceous carbonates (Fig. 2; Raić et al., 1980). Its SE extension offshore Šipan island is unclear. The frontal thrust of the Pelješac – Dubrovnik fault zone located to the SW of the Jakljan thrust is observed on 2D reflection seismics cross-sections offshore Pelješac and Elafiti islands as a blind fault covered by Pliocene-Quaternary strata deposited above the Messinian unconformity (Fig. 2b). The same structural-depositional relationship is seen along the profile A-A' further SW above and in front of the Mljet island structure, thus indicating that the activity of delineated offshore thrusts was the most intensive during Eocene-Oligocene and then decreased during Miocene and Pliocene-Quaternary times. A possible Pliocene-Quaternary activity of the frontal thrust of the Pelješac Dubrovnik fault zone has been observed on the 2D reflection seismic cross-sections in the offshore area of Koločep island. However, due to the limited extension and resolution of 2D reflection seismic cross-sections, it is not possible to clearly estimate about fault displacements.

3. Material and methods

3.1. Algal rims as sea-level markers

The *Lithophyllum* rim is a bioconstruction formed on rocky coasts by the coralline alga *Lithophyllum byssoides* slightly above the mean sea level (MSL) (Laborel et al., 1994; Faivre et al., 2013, 2019a, 2021a, 2021b). In sheltered microtidal environments, the alga yields accuracy of ±10 cm (Laborel and Laborel-Deguen, 1994; Faivre et al., 2010, 2013, 2019a, 2021a, 2021b; Blanfuné et al., 2016). Elevation was taken from the lowest living thalli of L. *byssoides,* the biological zero (Laborel, 1987; Laborel and Laborel-Deguen, 1994; Laborel et al., 1994) which in microtidal environments corresponds to the MSL with an accuracy of ≤0.1 m (Schembri et al., 2005; Stiros and Pirazzoli, 2008; Vacchi et al., 2016). Consequently, the error here has been further defined as ±15 cm. It should be noted that all internal errors within the dataset related to modern equivalents remain consistent at ±10 cm.

The indicative range associated with these sea-level index points (SLIPs) sensu van de Plassche, (1986a), Shennan (2015) or Vacchi et al. (2016) is from the Highest Astronomical Tide (HAT) to MSL.

Fixed biological markers like L. *byssoides* always occur within a well-defined elevation with respect to the tidal datum, however they do not always represent perfect horizontal lines. They may be naturally warped, by local hydrodynamic variations. Therefore, each individual altitudinal measurement has been done on a vertical profile of its own. This relates to the fossil specimens and to its present equivalents (Laborel, 1979; Stewart and Morhange, 2009). Large rims found in relatively sheltered conditions have the best potential for reconstructions of RSL change. This is the case for rims on Jakljan and Šipan islands.

3.2. Radiocarbon analyses

Samples were labelled, cleaned and dried. They were cut with a diamond saw in the Laboratory of Physical Geography at the Department of Geography (GEOLAB), Faculty of Science, University of Zagreb and then dated by the ^{14}C method. The accelerator mass spectrometry (AMS) ^{14}C technique was undertaken using graphite sample preparation in the Radiocarbon Laboratory at the Ruđer Bošković Institute in Zagreb (Krajcar Bronić et al., 2010) and ^{14}a measurement of graphite targets on AMS in the Center for Applied Isotope Studies, University of Georgia (USA).

Forty-one samples from the algal formation were dated. The ^{14}C ages are expressed by convention as ^{14}C years BP. The ages were calibrated using the standard MARINE20 calibration curve (Heaton et al., 2020) and the regional average marine reservoir correction (ΔR) for *Lithophyllum byssoides* from the Adriatic recalculated with MARINE20 (Faivre et al., 2015, 2019b). The MRE was obtained by analysing pre-bomb L. *byssoides* samples from the Adriatic revealing a ΔR (weighted mean) value of −209 ± 35 ^{14}C yr (Faivre et al., 2019b). The ^{14}C ages were corrected for isotope fractionation and normalized to - 25‰ VPDB (Stuiver and Polach, 1977).

3.3. Stable isotope analyses

The stable isotope composition (δ^{18}O and δ^{13}C) of the 44 samples was analysed at the University of Melbourne, Australia (7) and the University of South Florida, USA (37). At Melbourne, samples of ~0.6–0.7 mg were weighed into septum-capped glass vials, which were then purged with ultra-high purity helium before being acidied with 0.05 mL of 105% orthophosphoric acid at 70 °C. The isotopic composition of the evolved CO_2 was measured using an Analytical Precision AP2003 continuous-flow isotope ratio mass spectrometer. Samples were normalized to the VPDB scale using reference materials as described in Tzedakis et al. (2018). Measurement uncertainty was 0.05‰ for C and 0.10‰ for O. At Florida, δ^{13}C and δ^{18}O were measured with a ThermoFisher MAT253 stable isotope ratio mass spectrometer coupled to a GasBench-II peripheral in continuous-flow mode located at the University of South Florida College of Marine Science Stable Isotope Biogeochemistry Laboratory. Measurement followed established procedures (Révész and Landwehr, 2002; Spötl and Vennemann, 2003). Secondary reference materials (TSF-1 δ^{13}C = 1.95 ± 0.05‰, δ^{18}O = −2.20 ± 0.06‰; Borba δ^{13}C = 2.87 ± 0.05‰, δ^{18}O = −6.15 ± 0.09‰; LECO-carb δ^{13}C = −15.45 ± 0.16‰, δ^{18}O = −20.68 ± 0.16‰, all calibrated with NBS19, NBS18 and LSVEC certified reference materials) were used to normalize measurements to the VPDB scale. Isotope ratio values are expressed in δ (‰) = $[(R_{sample} / R_{standard}) - 1] \times 1000$.

3.4. Quantitative analyses of relative sea-level changes

Data obtained from the Jakljan and Šipan algal rims form a time series with an uneven distribution of measured points and with vertical and temporal uncertainties. We used an Error-In-Variables Integrated Gaussian Process (EIV-IGP) model (Cahill et al., 2015) to quantify the RSL changes at Jakljan and Šipan islands. Based on this approach, we have calculated RSL trends and rates with 95% confidence intervals. Thus, to account for vertical RSL uncertainties, a Gaussian process (GP) (Williams and Rasmussen, 1996) was used to model rates of RSL change, whereas its integral (integral of the Gaussian process, IGP) was used to model RSL change. IGP was set in an error-in-variables (EIV) framework to account for temporal uncertainties (Devy et al., 2000).

The Adriatic GMSL curve was constructed using previously published data from Istria in the Northern Adriatic (3 sites) (Faivre et al., 2019a), from the southern Adriatic island of Lopud (Faivre et al., 2021a) and the Jakljan dataset (this study). The GMSL was reconstructed using a total of 80 sea-level index points from six Adriatic algal rim structures corrected for site-specific GIA and tectonic effects. We subtracted a constant subsidence rate from the records, assuming that a steady rate is suitable for this time period, considering the Earth's viscoelastic response (Peltier, 1996; Kemp et al., 2015, 2018).

We transformed the Adriatic GMSL and northern Adriatic δ^{18}O datasets using a Loess smoothing (with a LOWESS algorithm) and performed a bootstrap to estimate a 95% confidence band based on 1000 random replicates. A regular interpolation (10-yr) was applied to the dataset. The Loess curve and the 95% confidence band were used as a proxy for Adriatic GMSL and Northern Adriatic δ^{18}O. The long-term trends were calculated using a moving average function (200-yr). We underlined the frequency distributions using a normal Fit (parametric estimation) and Kernel density estimation.

The periodicity of the Adriatic GMSL was studied using a wavelet analysis (wavelet transform) with Morlet as the basis function. The scalogram is displayed as periods against a linear age-scale. The cone of influence marks the increasing importance of the edge effects. Sinusoidal regressions were used in order to model periodicities in the time-series (the P_{value}, based on an F test, gives the significance of the fit). The three main periodicities were then selected to highlight the long-term trends in Adriatic GMSL. A Loess smoothing (with a LOWESS algorithm) and a 95% confidence band were added. The same process was applied to northern and southern Adriatic $\delta^{18}O$ datasets.

The relationship between Adriatic GMSL and southern Adriatic $\delta^{18}O_w$ (Siani et al., 2013) was tested, ranking the southern Adriatic $\delta^{18}O$ scores in ascending order and retaining the associated Adriatic GMSL scores. The two datasets are plotted with their confidence intervals (95%). The long-term trends are based on linear and polynomial models ($P_{value} < 0.001$). The Adriatic GMSL and southern Adriatic $\delta^{18}O$ were also cross-correlated to ascertain the best temporal match. The correlation coefficient (R^2) is given, focusing on the Lag_0 value (with +0.50 and − 0.50 as significant thresholds).

4. Results

4.1. Relative sea-level change at Jakljan and Šipan islands

4.1.1. Jakljan algal rim

Jakljan algal rim (N 42.444, E 17.485) is 14 m long and up to 180 cm wide (Fig. 3). It follows a 30–210° oriented fracture zone. Two distinct levels can be observed: the lower one ending at around −50 cm below current MSL and the upper one, ending at ~MSL. This algal rim started to form at 170 cal BC, 80 cm below present MSL. Until 540 cal AD, the RSL rates fluctuated between 0.26 and 0.39 mm/yr yielding a mean modelled rate of 0.36 mm/yr, then fell until 1210 cal AD at a rate of 0.19 mm/yr. RSL then rose at a mean rate of 0.31 mm/yr up to the beginning of the 19th century (1837 cal AD) (Fig. 3).

Between 980 and 1590 cal AD, no data were obtained pointing to a break in algal rim formation. Between ~1600 cal AD up to 1800 cal AD, RSL rose at a mean rate of ~0.48 mm/yr while after 1900 cal AD the rates exceeded 0.87 mm/yr.

The particularly thick and hard lower-level algal rim testifies to good rim building conditions between 170 cal BC and ~ 980 cal AD period (lasting ~1200 years), which formed under a mean rate of RSL change of 0.32 mm/yr. The upper part of the rim was formed under higher rates of ~0.48 mm/yr, and is extremely brittle.

4.1.2. Šipan algal rim

Šipan algal rim (N 42.419, E 17.544) is up to 130 cm wide at its most protruding part and it is ~9 m long. On the opposite side of the bay, the rim is up to 70 cm in width (Fig. 4). The rim extends in a NW-SE direction (140–320°) in accordance with major delineated faults and bedding (Fig. 2). The oldest sample has been attributed to 367 cal AD, found 70 cm below MSL (Fig. 4, Table 1), but the obtained data further fluctuate between −80 and − 60 cm below MSL pointing to possible discontinuities, which are within the measurement uncertainty. The lower-level rim is not developed, and only small patches are present. Until ~900 cal AD the modelled rates of RSL change vary from 0.28 to 0.45 mm/yr. For the following period of around 300 years (935–1270 cal AD), no data on algal rim formation have been obtained.

From 1270 cal AD, a large sturdy rim starts to develop, pointing to the establishment of good rim-building conditions at this site. From ~1270 till 1678 cal AD the RSL rose at a mean modelled rate of 0.39 mm/yr. Close to 1667 cal AD, a small discontinuity is noticed

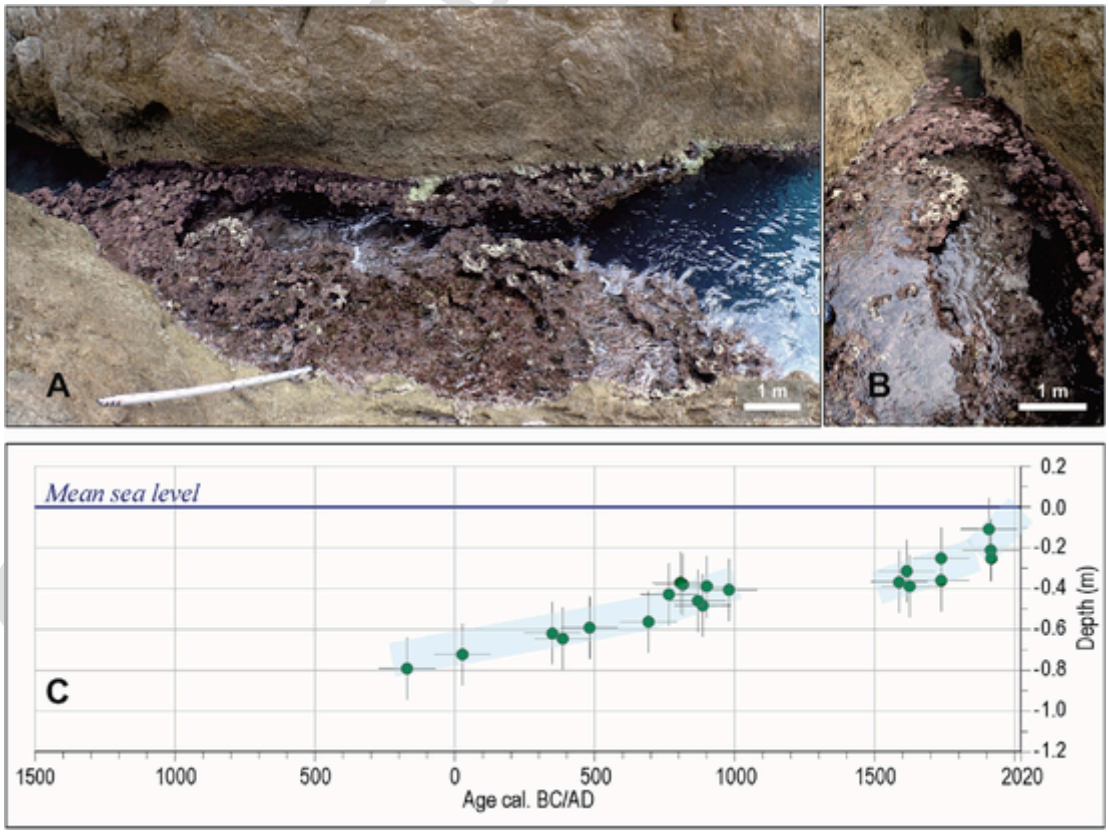

Fig. 3. Relative sea-level change at Jakljan island; A) and B) algal rim, C) 2.2 ka Relative sea-level curve derived from the algal rims - green circles. Error bars correspond to two standard deviations (2 s). Blue band represents segmented linear trendlines. (For interpretation of the references to colour in this figure legend, the reader is referred to the web version of this article.)

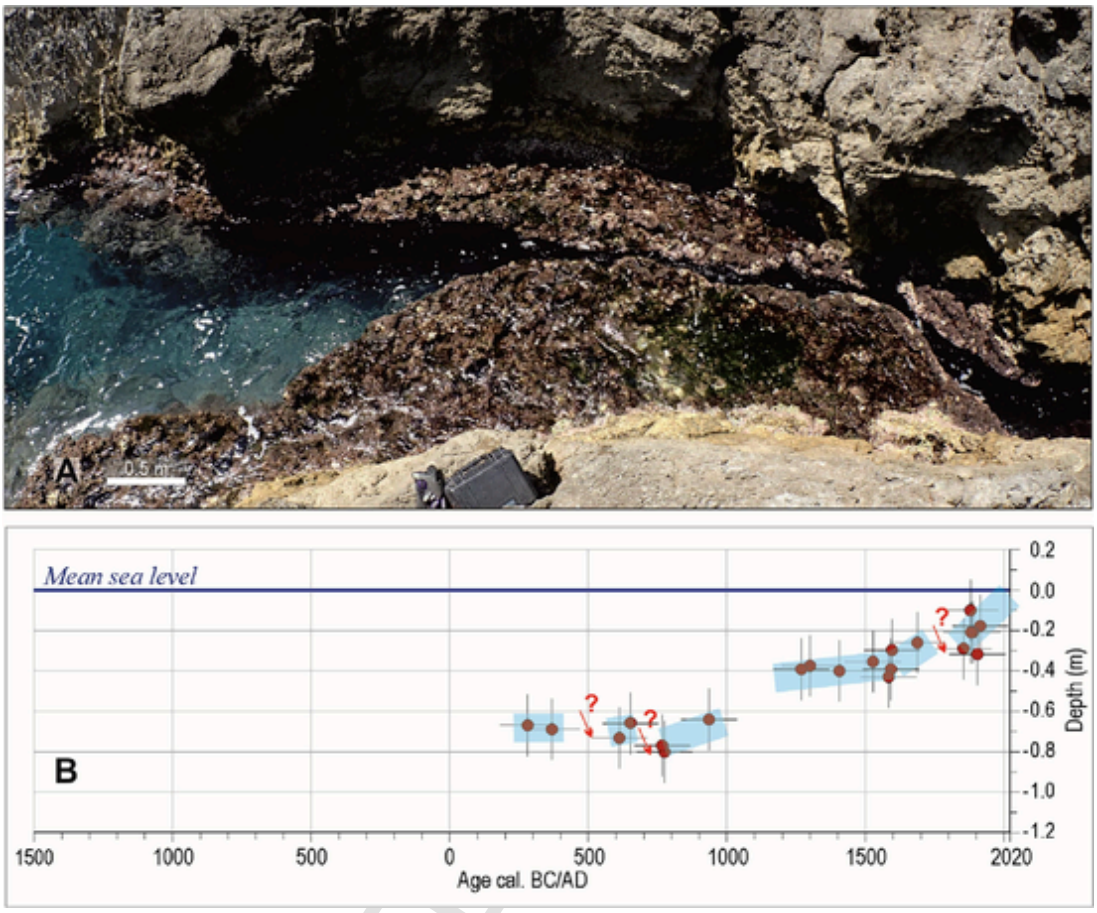

Fig. 4. Relative sea-level changes at Šipan island; A) algal rim; B) 1.8 ka RSL curve derived from the algal rims - red circles. Error bars correspond to two standard deviations (2 s). Blue band represents segmented linear trendlines. Red arrows mark periods of abrupt RSL change i.e. potential coseismic events. (For interpretation of the references to colour in this figure legend, the reader is referred to the web version of this article.)

pointing to a possible RSL fall (Fig. 4). After 1890 cal AD, the rates of RSL change increased significantly and attained a mean rate of 0.88 mm/yr, increasing to 0.93 mm/yr during the most recent period.

4.2. Distinction between regional GIA values and global-scale contributions at Jakljan

The availability of new high-resolution sea-level index points from the island of Lopud in the Southern Adriatic allowed us to estimate the regional GIA values. Field evidence from Lopud revealed a recent GIA rate of around 0.34 mm/yr (Faivre et al., 2021a). To distinguish global from regional processes, we subtracted GIA from the local RSL curves. Due to estimated coseismic movements of small magnitude (within the error bars) which affected Šipan island (Fig. 4), only Jakljan data are used. Consequently, we removed the linear regional contributions from the 2.2 ka Jakljan RSL curve.

The obtained sea level curve corrected for regional linear GIA effects showed that Jakljan GMSL varied between −0.01 m and − 0.20 m (Fig. 5a), i.e. ~20 cm in 2.2 ka. Between 180 cal BC and 1880 cal AD, the EIV-IGP modelled sea-level rates fluctuated between −0.29 and 0.42 mm/yr. From 45 to 450 cal AD sea level rates first decelerated and further rose at a mean rate of 0.01 mm/yr (Fig. 5). Between 450 and 1100 cal AD sea level fell at a rate of −0.10 mm/yr, but between 950 and 1100 cal AD the sea-level drop accelerated at a mean rate of −0.26 mm/yr. Sea-level rates further decelerated and started to increase at Jakljan after 1590 cal AD at a mean modelled rate of 0.1 mm/yr (Fig. 5).

4.3. Stable isotope composition of algal samples ($\delta^{13}C$ and $\delta^{18}O$) at Jakljan and Šipan

The $\delta^{13}C$ and $\delta^{18}O$ stable isotope values from Jakljan and Šipan algal samples correlated at $R^2 = 0.98$ and 0.95 respectively, allowing us to assume that precipitation occurred under isotopic equilibrium (Leng and Marshall, 2004; Talbot, 1990; Faivre et al., 2019b).

The obtained $\delta^{13}C$ values for all algal samples, from Šipan and Jakljan sites represent standard ranges for marine carbonates (Table 1; Fig. 6). Before the Industrial era, $\delta^{13}C$ values ranged between 2.87 and 3.14 ‰ and exhibited a mean value of ~1.7 ‰ in the study area. Recent records revealed an important decrease to −2.87 ‰.

The $\delta^{18}O$ records at Šipan and Jakljan sites range from 1.26 to 2.00 ‰ (Fig. 6; Table 1) with a mean of 1.73 ‰ for the pre-industrial era. The highest $\delta^{18}O$ values were recorded between 800 and 870 cal AD (~2.00 ‰ at 815 cal AD) and during different periods of Little Ice Age (LIA) principally in its first part, at ~1527 cal AD (1.92 ‰) and ~ 1612 cal AD (~1.97 ‰). Recent $\delta^{18}O$ records show very low negative values (−1.32 ‰, Table 1). Periodic minor decreases in both $\delta^{13}C$ and $\delta^{18}O$ values also occurred at around 935, 1300, 1595 and 1885 cal AD consistent with warmer periods (Table 1, Fig. 6).

4.4. Adriatic GMSL signal and its driving forces

The overall GMSL signal extracted from the northern and southern Adriatic algal rim data have revealed low mean amplitude variations of ±10 cm (Fig. 7) related to global climate effects. Therefore, we first tested our GMSL records for external (solar) forcing which could under-

Table 1
Radiocarbon dates obtained on *Lithophyllum byssoides* samples from Šipan (Š) and Jakljan (J) rims.

Z-	Sample	$\delta^{13}C$ ‰ VPDB	$\delta^{18}O$ ‰ VPDB	^{14}C age (yr BP)	σ	Cal ^{14}C age BC/AD Median	Height in relation to MSL (cm) ±15	Calibrated range (cal BC/ cal AD), 2σ
	Šipan							
–	Š0rec	−2.87	−1.32	–	–	2016	–	–
7253	Š19a	2.444	1.516	217	15	1913	−17.5	1834–modern
7254	Š20b	2.597	1.685	301	15	1905	−32	1804–modern
7591	Š20g	2.228	1.425	353	22	1887	−21	1915–modern
7259	Š6n	2.036	1.636	346	21	1884	−21	1915–modern
6637	Š3_1	2.15	1.65	336	23	1883	−10	1914–modern
7590	Š20e	2.596	1.707	423	22	1853	−29	1710–modern
7258	Š6k	2.868	1.812	592	22	1687	−26	1520–1859
7257	Š6i	2.716	1.643	678	21	1598	−29.5	1459–1752
6638	Š6A_4	1.87	1.26	683	22	1594	−39	1455–1746
7260	Š6A_2	2.418	1.623	699	22	1582	−43	1444–1718
7256	Š6e	2.595	1.918	765	22	1527	−35.5	1412–1666
7255	Š6a	2.805	1.651	911	22	1402	−40	1288–1521
7324	Š6c	2.087	1.560	1047	22	1299	−37.5	1169–1428
7645	Š6b	2.694	1.613	1081	22	1267	−39	1126–1409
6642	Š8_8	2.02	1.41	1414	22	935	−64	775–1087
6639	Š9A_1	2.81	1.54	1566	22	776	−80	647–937
6640	Š8_1	2.74	1.55	1574	23	768	−77	639–929
7262	Š8_6	2.619	1.784	1692	22	653	−66	501–802
7261	Š8 2_b	2.994	1.880	1733	22	612	−73	454–753
6641	Š8_4	2.54	1.52	1961	22	365	−69	214–542
7793	Š8_5	2.706	1.897	2037	22	280	−67	112–439
	Jakljan							
–	J0rec	−1.69	−0.66	–	–	2016	–	–
7313	J6_13	2.602	1.547	150	22	1915	−21	1844–modern
7314	J6_9b	2.618	1.710	45	23	1916	−25	1858–modern
7273	J6_17	2.753	1.728	243	22	1911	−11	1826–modern
7272	J6_9	3.051	1.790	553	22	1734	−25	1554–1904
7648	J6.4	3.090	1.879	553	22	1734	−35.5	1554–1904
7271	J6_1	3.037	1.735	650	22	1623	−38.5	1481–1794
7315	J6_5	2.995	1.969	661	23	1612	−31	1471–1779
7647	J6.3	2.965	1.859	696	22	1584	−36.5	1445–1722
7316	J8_d	3.144	1.882	1372	26	978	−40.5	818–1147
7318	J10_e	2.953	1.861	1448	23	900	−39	735–1045
7317	J8_a	2.956	1.728	1464	23	883	−48	722–1030
7650	J8_b	3.072	1.931	1477	22	869	−46	712–1019
7646	J10f	3.058	2.001	1528	23	815	−38	674–973
7649	J10h	2.908	1.946	1535	23	808	−37	633–923
7319	J10_c	2.982	1.750	1577	23	766	−42.5	633–923
7320	J11_f	3.147	1.877	1655	22	691	−56	555–842
7275	J11_d	2.871	1.869	1865	22	479	−59	323–639
7321	J12_o	3.033	1.774	1946	23	383	−64.5	230–554
7274	J11_b	2.892	1.892	1976	22	348	−62	191–526
7322	J12_i	2.818	1.774	2246	23	24	−72	cal 151 BCE–cal 201 CE
7323	J12_b	2.978	1.874	2396	23	169 cal BC	−79	cal 349 BCE–cal 4 CE

pin Adriatic GMSL variations. The analyses show the occurrence of ~350-year Grand Solar Cycles in the Adriatic GMSL records. Other, shorter cycles such as DeVries–Suess and Gleissberg cycles (Fig. 8a) can also be detected. The Late Antique LIA, Oort, Wolf, Spörer and Maunder minima can be further distinguished in the Adriatic sea-level records (Fig. 8b).

The $\delta^{18}O$ and $\delta^{13}C$ data show weak variability in the Southern Adriatic up to the Current warm period (Fig. 6), compared to the more continental Istria (Fig. 7b). Therefore, we here test the $\delta^{18}O$ curve from the Northern Adriatic (Istria) (Fig. 7b) ranging from −1.7 to 2.2‰ VPDB (Faivre et al., 2019a) towards the Adriatic GMSL variations. Three main periodicities are found indicating that SST variations are centred on 700-year, 350-year and 220-year cycles. However, the 350-year cycle dominates (Fig. 8c).

We further analysed the periodicities of the GMSL in relation to a salinity record derived from the oxygen isotope composition of seawater ($\delta^{18}O_w$) from a sediment core collected in the Southern Adriatic (Siani et al., 2013). Two main periodicities are observed: one at 200 yr and one at 350 yr, which are consistent with our previous observations (Fig. 9).

To establish a closer link between the GMSL variation and salinity, a cross-correlation was calculated (Fig. 9c), assessing the temporal correspondence between the two time series using the correlation coefficient. Here we found that the GMSL rise is negatively correlated with the increase in salinity (Lag_0–0.78, Pvalue <0.001). The increase in salinity could therefore be related to the periods of RSL drop (Fig. 9).

5. Discussion

5.1. Late Holocene relative sea-level trends at the Elafiti islands (Southern Adriatic)

The RSL reconstruction on Jakljan island shows ~80 cm of RSL rise since 170 cal BC (Fig. 3) with an EIV-IGP modelled average RSL change rate of 0.33 mm/yr. On Šipan, there has been ~70 cm of RSL rise since 367 cal AD (Table 1) at a mean modelled rate of 0.45 mm/yr. This difference derives from local non-linear contributions observed only on Šipan (discussed in chapter 5.2). The 2 ka rates at Jakljan correspond to those previously observed at nearby Lopud, Koločep and Grebeni islands (after correction for local tectonic contributions) which generally vary between 0.3 and 0.4 mm/yr and where the rates attain 1.4 mm/yr after 1800 cal AD (Faivre et al., 2021a, 2021b). The ~0.3–0.4 mm/yr rates are close to the regional glacial -isostatic adjustment (GIA) estimates of 0.34 mm/yr observed at Lopud island (Faivre et al., 2021a), as well as to the model predictions of Stocchi and Spada (2009) and Lambeck et al. (2011) (ICE-5G (RVM2) and K33_j1b_WS9_6, respectively).

5.2. Tectonic controls on local sea-level variations: late Holocene evidence from the Elafiti islands

The RSL histories of Jakljan and Šipan differ slightly. We assume that these differences are related to local tectonic contributions. The coasts of Jakljan do not provide evidence for late Holocene tectonic uplift. Consequently, the fault interpreted by Šolaja et al. (2022, their figure 13) along the southwestern coast of Olipa and Jakljan islands does not seem to be active in the last 2 ka. However, cosesmic movements are present on Šipan island where several consecutive low magnitude displacements are observed. Within the measurement uncertainty of ±15 cm, these displacements correlate well with previously attested uplift events along the Pelješac - Dubrovnik fault zone (Faivre et al., 2021a, 2021b).

The first observed displacement relates to one of the two events: the 367 or 522 CE earthquake(s) while the second refers to the 650–800 cal AD period that could be related to the 750–1100 cal AD event previously defined at Lopud, Koločep and Grebeni (Faivre et al., 2021a, 2021b). Archaeological excavations at the Fort Sokol site in the Konavle area (about 45 km SE from Šipan) provide additional evidence

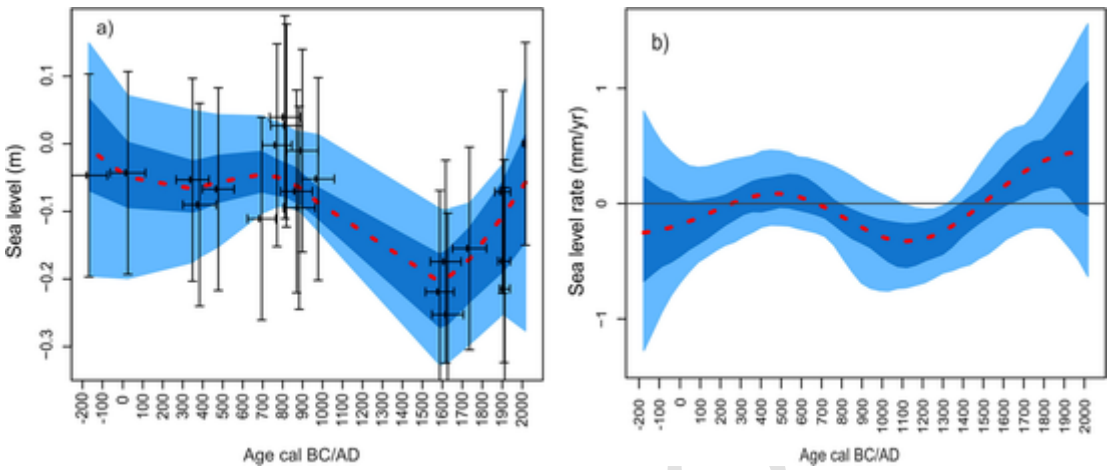

Fig. 5. A) GIA adjusted sea-level change for Jakljan Island, EIV-IGP model predictions (mean (dashed red lines) with 68% (dark blue) and 95% (light blue) confidence intervals); B) Estimated rates of sea-level change after GIA correction. (For interpretation of the references to colour in this figure legend, the reader is referred to the web version of this article.)

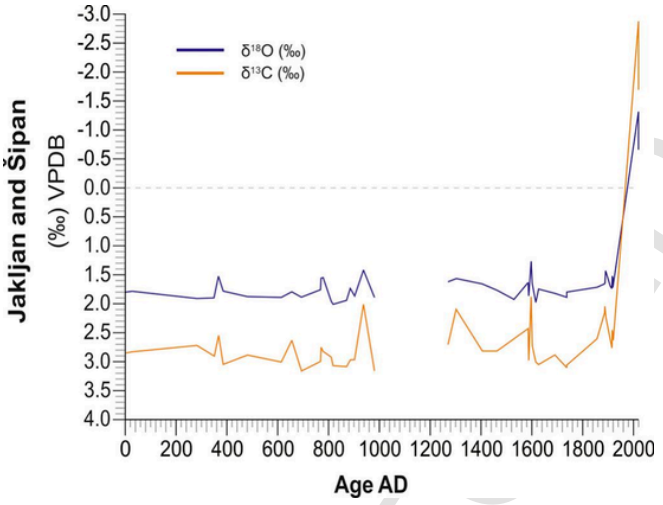

Fig. 6. Stable isotopes records from the Šipan and Jakljan algal rims.

for several destructive earthquakes, which preceded construction of the graves dated to the 6th and 7th centuries (Topić et al., 2019).

Assumed small consecutive uplifts on the island of Šipan probably led to erosion of the alga close to the intertidal zone. As a result, the lower-level algal rim could not develop, and only small patches were observed. Thus, local tectonic effects caused the morphological differences between the Jakljan and Šipan island rims.

Later, at 1690 cal AD a small discontinuity is again observed (~5 ± 15 cm), which could be tentatively related to the great Dubrovnik earthquake of 1667, one of the largest events in the External Dinarides during the last millennium and which, according to historical evidence, was felt on Šipan, but did not cause significant damage (Kišpatić, 1891). Nearby Jakljan island is uninhabited, so historical data are absent.

Therefore, we assume that the Šipan segment of the fault is active with uplift episodes of 10–15 ± 15 cm per event and that several earthquakes ruptured the main Pelješac-Dubrovnik frontal thrust fault from Šipan to Grebeni islands in the last 2 ka, decreasing in magnitude with time as also observed at Koločep and Grebeni (Faivre et al., 2021b). The estimated total uplift of 20–25 cm in 1.6 ka provides uplift rates of ~0.1–0.2 mm/yr (Fig. 10).

The data reveals a pattern of increasing uplift amplitude per event towards the southeast, with Šipan showing an uplift of 10–15 ± 15 cm, followed by Lopud with 15–45 ± 15 cm, and Koločep and Grebeni exhibiting the highest uplift of 40–60 ± 15 cm. Thus, the data obtained from the rims indicates that there is an uplift along the Pelješac-Dubrovnik fault zone, with increasing rates from Šipan to Grebeni, ranging from 0.1 to 0.2 mm/yr to 0.6–0.8 mm/yr, respectively (Fig. 10). These uplift rates correspond to the fault slip rates of 0.1–1.5 mm/y modelled by Kastelic et al. (2013) for the frontal thrust of the Pelješac – Dubrovnik fault zone (their Pelješac – Kotor composite seismogenic source).

5.3. Variations in the GMSL signal at Jakljan (Southern Adriatic)

The global sea-level component derived from Jakljan in the Southern Adriatic reveals low amplitude variations up to 20 cm corresponding to previous observations at Lopud (Faivre et al., 2021a) and to 2 ka mean global variations (Kopp et al., 2016; Kemp et al., 2018; Walker et al., 2021).

According to the EIV-IGP modelled data, from 45 until 450 cal AD, the GMSL component was relatively stable (Fig. 5). Furthermore, between 450 until 1100 cal AD, the Southern Adriatic GMSL fell at mean modelled rates of −0.10 mm/yr matching the GMSL signal found by Walker et al. (2021). However, after 1000 cal AD sea level fell at much faster rates exceeding −0.26 mm/yr (going up to −0.28 mm/yr) (Fig. 3), similar to values reported by Kopp et al. (2016) (−0.2 ± 0.2 mm/y over 1000–1400 CE) and Kemp et al. (2018) (at 1000–1200 CE).

As the Jakljan 2.2 ka RSL data does not show any local coseismic displacements, and the regional GIA component is assumed to be linear, the temporal hiatus in algal rim formation at Jakljan island indicates a significant change in GMSL contribution after approximately ~1000 cal AD (Fig. 3). The sea-level slowdown is clearly attested in all RSL curves from the Southern Adriatic after ~750–800 cal AD (Figs. 3, 7), while the absence of rim data (only one data point, Fig. 10) between ~1000–1250 cal AD at all studied sites on Elafiti further supports the assumption of an accelerated sea-level fall. Thus the drop in global sea-level contribution likely caused the cease of algal rims formation on all Elafiti islands, as regional GIA rates were cancelled-out by the GMSL fall.

During the period 1270–1500 cal AD, the mean modelled RSL rates began to rise. The rim started to form at Šipan, while at Jakljan, growth became evident only after ~1590 cal AD when the RSL rates attained ~0.30 to 0.35 mm/yr, i.e., according to our previous work, best conditions for algal rim formation. The formation of the rim on Šipan island initiates around 1270 cal AD, aligning with the findings from all surveyed sites in Elafiti (as shown in Fig. 10) and corroborated by the sta-

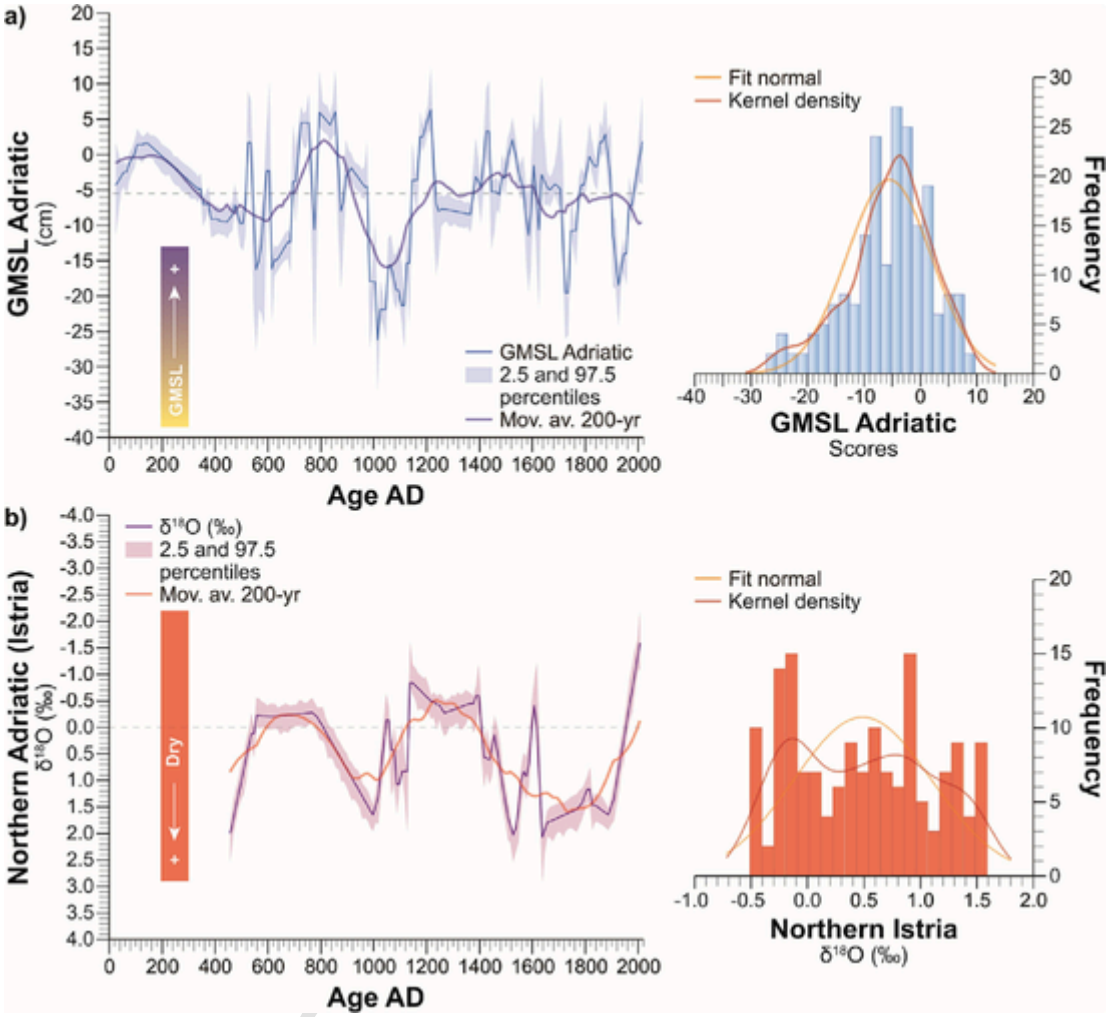

Fig. 7. a) Variation of global mean sea-level contribution (GMSL) from the Adriatic during the last two millennia. b) Northern Adriatic $\delta^{18}O$ ‰ VPDB records from algal rim structures (Faivre et al., 2019a). The two curves are shown with a 95% confidence band (2.5 and 97.5 percentiles). The long-term trends are depicted as a 200-yr moving average. The frequency distributions are portrayed with a normal Fit and Kernel density estimations.

ble isotope signature exhibiting lower $\delta^{18}O$ values (Fig. 6). This collective evidence suggests that the significant transition leading to rim formation in the Elafiti region likely occurred between 1250 and 1300 cal AD. This is in accordance with the change point defined in Walker et al. (2021). Therefore, at Jakljan the data may not have precisely captured the very beginning of the rim growth after the break.

The temporary break in algal rim formation thus resulted in rims of particular morphology i.e., in formation of rims with two pronounced levels. This particular morphology was previously observed on Vis and Biševo islands (Faivre et al., 2013). On Jakljan island, where no local tectonic contributions have been observed, the algal rim formed until the velocity of the modelled RSL change dropped below ~0.1 mm/yr, pointing to velocities generally needed for the algal rim formation.

5.4. Variation of the Adriatic GMSL signal and its driving forces

The obtained Adriatic GMSL curve reveals several phases of RSL drop during the last 2 ka. Two of them are clearly observed in the algal rim data, though, the most important occurred at ~1000 cal AD related to the cooler period corresponding to the Oort Minimum, a phase of low solar activity (Yiou et al., 2012), from 1000 ± 40 to 1050 ± 40 CE (Kaniewski et al., 2022). Until now, the Oort Minimum had not been described as a major event in the Northern Adriatic (at Aquileia or in the Gulf of Venice, Kaniewski et al., 2022; Camuffo et al., 2000) however, it could be linked to the heaviest $\delta^{18}O$ values observed in Istria (Fig. 7b) (Faivre et al., 2019a). Consequently, the sea-level drop may have been expedited by the impacts of the solar minimum.

This GMSL drop could thus be related to the Northern Hemisphere global mean cooling attested by Moberg et al. (2005), Mann et al. (2008), Ljungqvist (2010), PAGES 2k Consortium (2013), Neukom et al. (2019), and a drop in Mediterranean SST (from ~800 till 1100 cal AD) (Marriner et al., 2022), but also in local speleothem $\delta^{18}O$ records from the Zadar area (Rudzka et al., 2012).

The early part of the Little Ice Age (~1400 to 1600 CE) was characterized by heightened variability, which led to unstable environmental conditions in both the Southern and Northern Adriatic regions (Faivre et al., 2019a; Kaniewski et al., 2022). The beginning of the 16th century was characterized by cold conditions (~1527 cal AD) (Table 1), but temperatures later increased, both in the Southern and Northern Adriatic (Figs. 6, 7b). This warmer phase is well recorded at Aquileia (from 1520 ± 40 to 1600 ± 30 CE), with an average annual temperature anomaly of 0.71 ± 0.15 °C (Kaniewski et al., 2022), corresponding to warm anomalies around ~1560 CE (Neukom et al., 2019). This warm period is correlated with a major increase in total solar irradiance (Steinhilber et al., 2009), and higher temperatures along the Croatian coast (Kaniewski et al., 2021). During this same period, there was a corresponding increase in GMSL in the Adriatic (Fig. 7). This trend was also reflected in the uniform GMSL signal observed in global datasets (Kopp et al., 2016; Kemp et al., 2018; Walker et al., 2021).

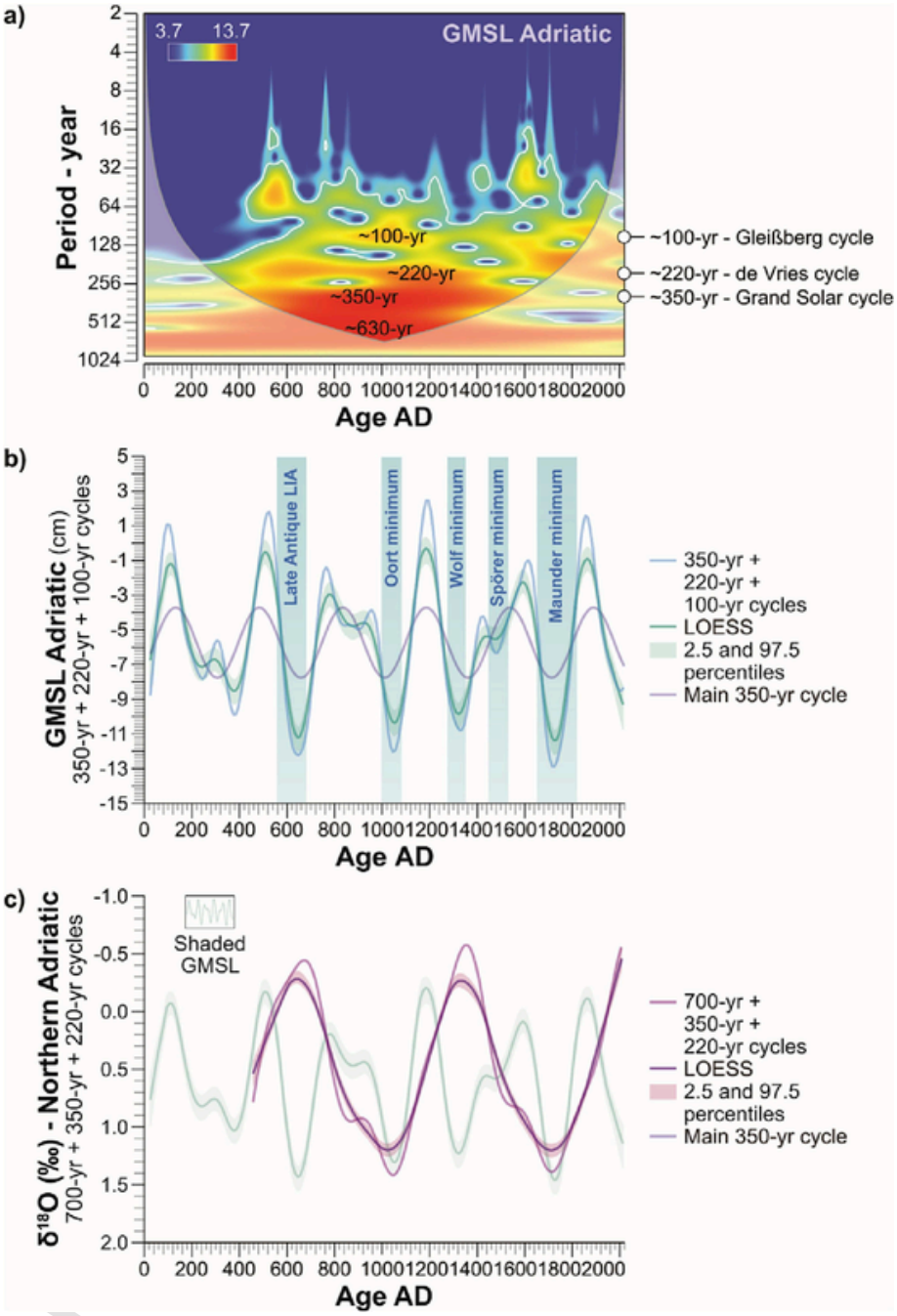

Fig. 8. Periodicity of the GMSL signal in the Adriatic during the last 2000 years in relation to: a) solar activity; b) low solar irradiance periods; and c) $\delta^{18}O$ ‰ VPDB variations in the Northern Adriatic (Faivre et al., 2019a). The wavelet analysis (scalogram) for GMSL Adriatic is detailed. The cone of influence is depicted as a grey line, and the significance level ($P = 0.05$) as white lines. Long-term trends are depicted as sinusoidal regressions with Loess smoothing (with the 2.5 and 97.5 percentiles).

The coldest phase of the Little Ice Age (LIA), which occurred in the later part of the period, in 1612 cal AD, is associated with a VPDB value of 1.97 ‰ (Fig. 7) for the Southern region. This aligns with the coldest observations in 1.5 ka recorded in the Northern region around 1600 cal AD, with a corresponding VPDB value of 2.22 ‰ (Fig. 7b). All the data from the Adriatic reveal cold conditions that could be related to the Maunder Minimum (Fig. 7) (1645–1715 CE; Shindell et al., 2001; Usoskin et al., 2015), in Aquileia covering the period from 1620 ± 30 to 1690 ± 30 CE (Kaniewski et al., 2022) and to the overall cool seventeenth century conditions (Neukom et al., 2019). Recent $\delta^{18}O$ and $\delta^{13}C$ records from the Adriatic (north and the south) show very low isotopic values that were not measured in the previous 2200 years (Figs. 6, 7b).

Furthermore, GMSL variability is strongly related to changes in salinity. Generally, changes in salinity are driven by the Adriatic wide-circulation regime that is controlled by the Bimodal Oscillating System (BiOS) (Gačić et al., 2010; Mihanović et al., 2015), the Northern Adriatic circulation (Cozzi and Giani, 2011; Djakovac et al., 2012) and is significantly affected by the Po river inflow (Dautović et al., 2017). However, decadal oscillations in salinity patterns are driven mostly by the BiOS and the Eastern Mediterranean Transient (EMT) system (Roether et al., 2007; Gačić et al., 2010, 2014).

The Bimodal Oscillating System (BiOS) closely link the dynamics of the southern Adriatic and Ionian Sea (Borzelli et al., 2009; Gačić et al., 2010). The upper-layer circulation in the Ionian Sea alternates at the

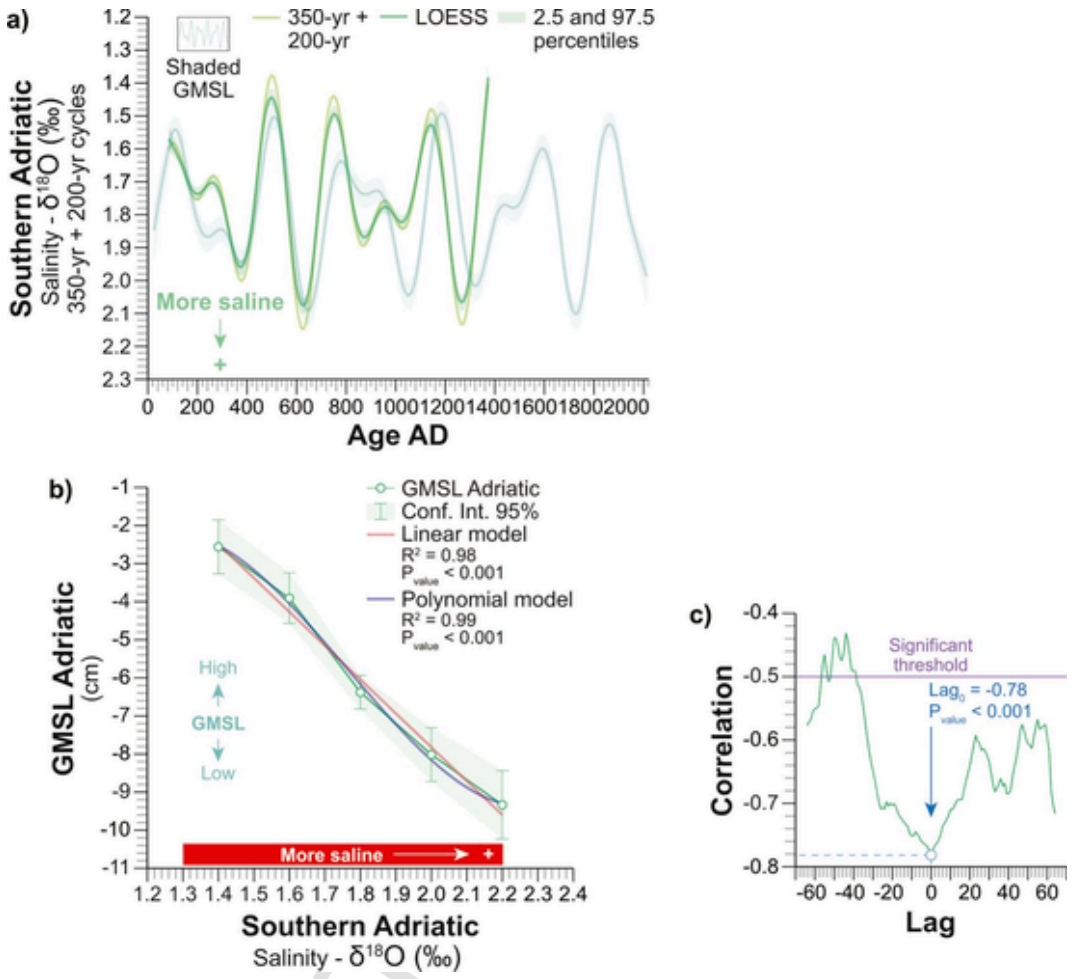

Fig. 9. Variations of Adriatic GMSL related to $\delta^{18}O_w$/salinity from the Southern Adriatic core (Siani et al., 2013); a) Periodicity, b) link between Adriatic GMSL and Southern Adriatic $\delta^{18}O$, with linear and polynomial models, and c) Cross-correlogram showing the link between GMSL and $\delta^{18}O_w$/salinity with the correlation coefficient at Lag_0 and the associated P_{value}.

decadal time scale, from anticyclonic to cyclonic and vice versa (Gačić et al., 2010; Mihanović et al., 2015). The alternation of circulation modes brings different water masses into the Adriatic, i.e. Modified Atlantic Water (MAW) during the anticyclonic Ionian circulation mode and Levantine Intermediate Water (LIW) during cyclonic Ionian circulation. During the cyclonic Ionian circulation mode (Gačić et al., 2010), there is a spread of Levantine high-salinity waters, making the Adriatic more prone to vertical convection and dense water production (Manca et al., 2002). During anticyclonic Ionian circulation patterns, inflow of relatively fresh waters into the Adriatic is favoured, increasing the buoyancy of the water column and obstructing the vertical convection. The anticyclonic mode also represents a preconditioning mechanism for dense water formation processes in the Aegean Sea and for possible Eastern Mediterranean Transient-like events (Gačić et al., 2011).

There is currently very limited information on the long-term changes in basin circulation, as well as on dense water formation intensity and the related strength of circulation patterns. Reconstructions cover approximately the last 60 years (Mihanović et al., 2015). However, several possible past EMT-type events have recently been proposed (at 1910 ± 12, 1812 ± 18, 1725 ± 25 and 1580 ± 30 CE), as determined by the link between surface water freshening (SCFR) in the Sicily Channel and enhanced deep-water ventilation in the Aegean Sea (Incarbona et al., 2016). During the SCFR episodes, we observed sea-level rise in the Adriatic (Fig. 7) suggesting weak mixing, low deep-water production and likely weakened circulation dynamics.

Periods of surface water freshening have also been observed in the southern Adriatic on longer time scales, at least during the last 6 ka, but especially between 3 and 0.6 ka (Siani et al., 2013) pointing to possible periods of reduced deep-water formation in the Southern Adriatic Sea and changes in thermohaline circulation in the Mediterranean. These oscillations reveal a possible link between periods of lower salinity in the Southern Adriatic Sea and periods of wetter climatic conditions in the northern and central Mediterranean (Siani et al., 2013).

Palaeoclimate studies provide indications on long-term salinity oscillations. Within the Adriatic GMSL record, we can distinguish alternating periods of generally higher salinity, lower temperatures and dry conditions related to periods of sea-level fall, from periods of generally low salinity, higher temperatures and more freshwater correlated with periods of sea-level rise (Fig. 9). Two main periodicities elucidated in the salinity signal are centered on 200-yr and 350-yr cycles.

Over the past 2000 years, fluctuations in the global mean sea level (GMSL) observed in Adriatic algal rims show a general correspondence in terms of magnitude, rate, and trend with previously published global signals (Fig. 11). While there may be a time lag of ~100 years (due to radiocarbon-dating uncertainty), the overall correspondence is notable. As shown in Fig. 11, increasing number of data points from Kopp et al., 2016 to Walker et al., 2021, curves become smoother (from 1345 to 2275, respectively). Consequently, higher variations in the Adriatic GMSL curve are expected.

The distinguished Adriatic GMSL signal could still include additional regional nonlinear steric effects associated with cooling phases

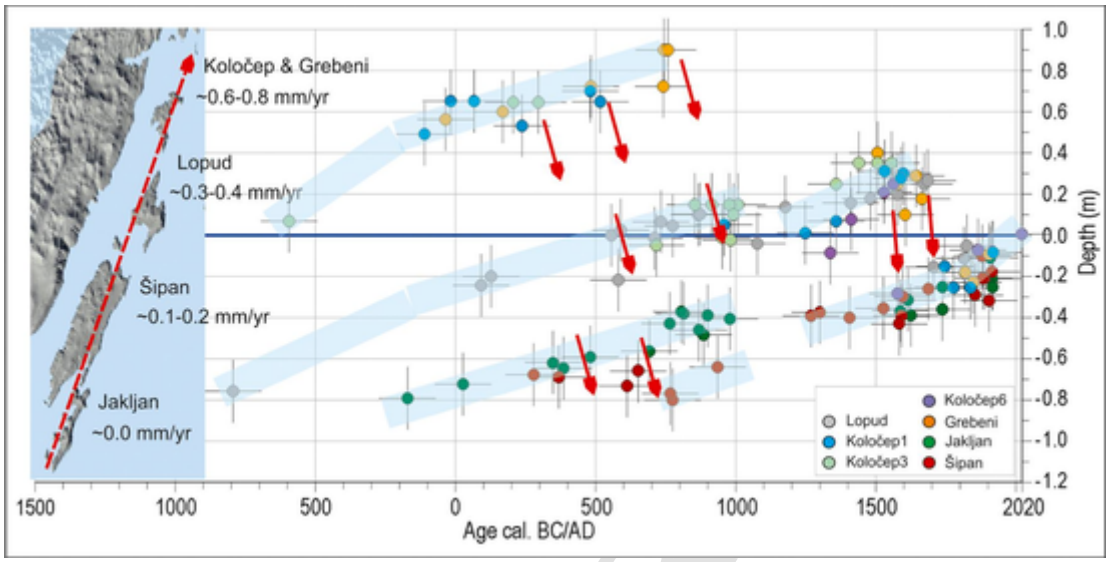

Fig. 10. Relative sea-level changes at the Elafiti islands (Lopud, Koločep, Grebeni – Faivre et al., 2021a, 2021b; and Jakljan and Šipan – this study) based on the geochronology of algal rims. Error bars correspond to two standard deviations (2σ). Blue band represents segmented linear trendlines. Red arrows mark periods of abrupt RSL fall i.e., possible seismic events. Left: dashed red arrow point to active coastal sectors in the past 1.6 ka with increasing uplift rates. Zero relates to the time of sampling at a particular location between 2016 and 2020. (For interpretation of the references to colour in this figure legend, the reader is referred to the web version of this article.)

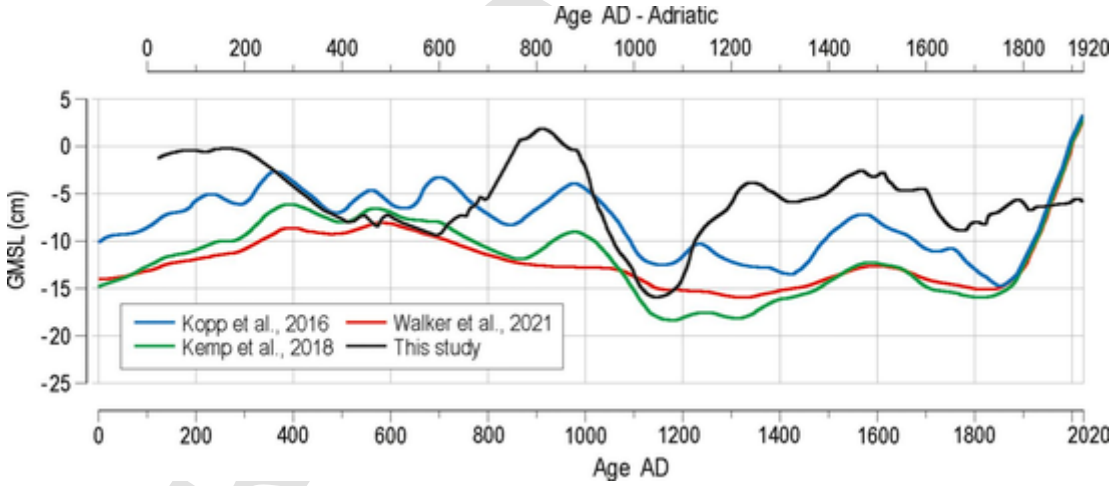

Fig. 11. Adriatic GMSL contribution related to GMSL cruves derived from global datasets (Kopp et al., 2016; Kemp et al., 2018; Walker et al., 2021).

(Roemmich and Gilson, 2009; Kemp et al., 2018) and also influences of atmospheric and ocean circulation (e.g. the strength of the North Atlantic Overturning Circulation) which can drive part of the regional sea-level changes (Kemp et al., 2018) and could account for differences between the Adriatic GMSL curve and GMSL signals obtained from global datasets.

6. Conclusion

The high-resolution proxy data obtained from *Lithophyllum rims* in the Adriatic allow us to distinguish major processes acting at different spatial and temporal scales during the past two millennia. We have elucidated their magnitudes, rates and trends at centennial to multidecadal timescales.

Local non-linear (coseismic) effects on the Elafiti islands in the Southern Adriatic were found to be a major process differentiating the RSL change between sites compared to the relatively uniform regional GIA effects and GMSL variations. The effects of coseismic uplift were shown to be absent on Jakljan (during the studied period), minor on Šipan, and maximal on Koločep and Grebeni (in a range from 0.1 to 0.2 mm/yr to 0.6–0.8 mm/yr, at Šipan and Grebeni, respectively). So, the data suggests that tectonic uplifting rates along the Pelješac-Dubrovnik fault zone may increase in a southeastward direction.

The algal-rim based GMSL curve for the northern and southern Adriatic (using 80 homogeneous RSL data points) have revealed two major periods of negative GMSL contribution. During these periods of increased GMSL drop at around ~1000 and ~ 1600 cal AD algal rims stopped forming as GMSL falls offset local rates of RSL rise. Even if the GMSL signal between −200 BCE to 1800 cal AD shows low-amplitude variations, temporary increased GMSL drops were significant enough to cancel out GIA rates or total land-level rates and thus influence algal rim growth and morphology. This increased GMSL drop >0.26 mm/yr at ~1000 cal AD corresponds to previous estimates of ~ −0.2 ± 0.2 mm/yr of Kopp et al. (2016) and Kemp et al. (2018).

Here we assessed the relationship between GMSL variability and solar forcing over the past 2 ka. Adriatic GMSL variations were mainly in phase with Grand Solar Cycles of ~350 years. The increased GMSL drop attested in algal rims occurred during the Ort and Maunder min-

ima, coinciding with decreases in SST, and with increases in surface water salinity. Consequently, the break in Adriatic algal rim formation during these periods resulted from negative climate-forced GMSL contributions.

Furthermore, the Adriatic GMSL curve roughly corresponds in magnitude, rates and trends to previously published GMSL signals obtained from global datasets (Kopp et al., 2016; Kemp et al., 2018; Walker et al., 2021). The observed differences between the Adriatic GMSL and mean global signals could be related to regional-scale steric effects as well as to changes in atmospheric and ocean dynamics.

Here we demonstrate that *Lithophyllum* rims can be used to improve knowledge of the driving mechanisms of relative sea-level changes at all scales providing evidence on GMSL variations, GIA, local tectonics, palaeoearthquakes and climate forcing. Thus, *L. byssoides* can provide a preindustrial baseline to help in understanding the patterns and causes of contemporary and future climate and sea-level changes as well as for the evaluation of future risks. Our results have important implications for future sea-level changes and also for future seismic hazard assessment in the Adriatic.

Declaration of Competing Interest

The authors declare that they have no known competing financial interests or personal relationships that could have appeared to influence the work reported in this paper.

Data availability

Data will be made available on request.

Acknowledgements

This research was supported by Croatian Science Foundation projects: HRZZ-IP-2019-04-9445 – Relative sea-level change and climate change along the eastern Adriatic coast – SEALeveL, HRZZ-IP-2013-11-1623, Reconstruction of the Quaternary environment in Croatia using isotope methods – REQUENCRIM and HRZZ-IP-2020-02-3960 – Characterization and monitoring of the Dubrovnik fault system - DuFAULT.

We greatly appreciate the field assistance of Donat Petricioli. We are also grateful to Srđan Čupić from the Hydrographic Institute of the Republic of Croatia for providing tide gauge data. We would also like to thank Ivica Rendulić and Marin Mićunović for help with illustrations.

Finally, we thank the two anonymous reviewers for their constructive comments that helped us to improve an earlier version of our manuscript.

References

Babić, Lj, Zupanič, J., 2008. Evolution of a river-fed foreland basin fill: the North Dalmatian flysch revisited (Eocene, outer Dinarides). Nat. Croatica 17 (4), 357–374.

Babić, Lj, Crnjaković, M., Asmerom, Y., 2012. Uplifted Pleistocene marine sediments of the central Adriatic Island of Brusnik. Geol. Croatic. 65 (2), 223–232. https://doi.org/10.4154/GC.2012.13.

Balling, P., Tomljenović, B., Schmid, S.M., Ustaszewski, K., 2021a. Contrasting along-strike deformational styles in the central external Dinarides assessed by balanced cross-sections: Implications for the tectonic evolution of its Paleogene flexural foreland basin system. Glob. Planet. Chang. 205, 103587. https://doi.org/10.1016/j.gloplacha.2021.103587.

Balling, P., Grützner, C., Tomljenović, B., Spakman, W., Ustaszewski, K., 2021b. Post-collisional mantle delamination in the Dinarides implied from staircases of Oligo-Miocene uplifted marine terraces. Sci. Rep. 11, 2685. https://doi.org/10.1038/s41598-021-81561-5.

Benetatos, C., Kiratzi, A., 2006. Finite-fault slip models for the 15 April 1979 (Mw 7.1) Montenegro earthquake and its strongest aftershock of 24 May 1979 (Mw 6.2). Tectonophysics 421, 129–143. https://doi.org/10.1016/j.tecto.2006.04.009.

Bennett, R.A., Hreinsdóttir, S., Buble, G., Bašić, T., Bačić, Ž., Marjanović, M., Casale, G., Gendaszek, A., Cowan, D., 2008. Eocene to present subduction of southern Adria mantle lithosphere beneath the Dinarides. Geology 36, 3–6. https://doi.org/10.1130/G24136A.1.

Blanfuné, A., Boudouresque, C.F., Verlaque, M., Beqiraj, S., Kashta, L.N.I., Ruci, S., Thibaut, T., 2016. Response of rocky shore communities to anthropogenic pressures in Albania (Mediterranean Sea): Ecological status assessment through the CARLIT method. Mar. Pollut. Bull. 109, 409–418. https://doi.org/10.1016/j.marpolbul.2016.05.041.

Borzelli, G.L.E., Gačić, M., Cardin, V., Civitarese, G., 2009. Eastern Mediterranean Transient and reversal of the Ionian Sea circulation. Geophys. Res. Lett. 36, L15108. https://doi.org/10.1029/2009GL039261.

Brunović, D., Miko, S., Hasan, O., Papatheodorou, G., Ilijanić, N., Miserocchi, S., Correggiari, A., Geraga, M., 2020. Late pleistocene and Holocene paleoenvironmental reconstruction of a drowned karst isolation basin (Lošinj channel, NE Adriatic Sea). Palaeogeogr. Palaeoclimatol. Palaeoecol. 544, 109587. https://doi.org/10.1016/j.palaeo.2020.109587.

Cahill, N., Kemp, A.C., Horton, B.P., Parnell, A.C., 2015. Modelling Sea-level change using errors-in-variables integrated Gaussian processes. Ann. Appl. Stat. 9, 547–571. https://doi.org/10.1214/15-AOAS824.

Camuffo, D., Secco, C., Brimblecombe, P., Martin-Vide, J., 2000. Sea storms in the Adriatic Sea and the western Mediterranean during the last millennium. Clim. Chang. 46, 209–223. https://doi.org/10.1023/A:1005607103766.

Cazenave, A., Palanisamy, H., Ablain, M., 2018. Contemporary Sea level changes from satellite altimetry: what have we learned? What are the new challenges? Adv. Space Res. 62, 1639–1653. https://doi.org/10.1016/j.asr.2018.07.017.

Ćosović, V., Mrinjek, E., Nemec, W., Španiček, J., Terzić, K., 2018. Development of transient carbonate ramps in an evolving foreland basin. Basin Res. 30 (4), 746–765. https://doi.org/10.1111/bre.12274.

Cozzi, S., Giani, M., 2011. River water and nutrient discharges in the Northern Adriatic Sea: current importance and long-term changes. Cont. Shelf Res. 31 (18), 1881–1893. https://doi.org/10.1016/j.csr.2011.08.010.

Dautović, J., Vojvodić, V., Tepić, N., Ćosović, B., Ciglenečki, I., 2017. Dissolved organic carbon as potential indicator of global change: a long-term investigation in the northern Adriatic. Sci. Total Environ. 587–588, 185–195. https://doi.org/10.1016/j.scitotenv.2017.02.111.

Dean, S., Horton, B.P., Evelpidou, N., Cahill, N., Spada, G., Sivan, D., 2019. Can we detect centennial sea-level variations over the last three thousand years in Israeli archaeological records? Quat. Sci. Rev. 210, 125–135. https://doi.org/10.1016/j.quascirev.2019.02.021.

Devy, D.K., Ghosh, S.K., Mallick, B.K., 2000. Generalized Linear Models: A Bayesian Perspective. Marcel Dekker, New York.

Djakovac, T., Degobbis, D., Supić, N., Precali, R., 2012. Marked reduction of eutrophication pressure in the northeastern Adriatic in the period 2000-2009. Estuar. Coast. Shelf Sci. 115, 25–32. https://doi.org/10.1016/j.ecss.2012.03.029.

Faivre, S., Butorac, V., 2018. Recently submerged tidal notches in the wider Makarska area (Central Adriatic, Croatia). Quatern. Int., Quatern. Croatia 494, 225–235. https://doi.org/10.1016/j.quaint.2017.07.020.

Faivre, S., Fouache, E., 2003. Some tectonic influences on the Croatian shoreline evolution in the last 2000 years. Zeitschrift für Geomorphol. N.F. 47 (4), 521–537. https://doi.org/10.1127/zfg/47/2003/521.

Faivre, S., Bakran-Petricioli, T., Horvatinčić, N., 2010. Relative Sea-level change during the late Holocene on the island of Vis (Croatia) - Issa harbour archaeological site. Geodin. Acta 23 (5–6), 209–223. https://doi.org/10.3166/ga.23.209-223.

Faivre, S., Fouache, E., Ghilardi, M., Antonioli, F., Furlani, S., Kovačić, V., 2011. Relative Sea level change in western Istria (Croatia) during the last millennium. Quat. Int. 232, 132–143. https://doi.org/10.1016/j.quaint.2010.05.027.

Faivre, S., Bakran-Petricioli, T., Horvatinčić, N., Sironić, A., 2013. Distinct phases of relative sea level changes in the central Adriatic during the last 1500 years - influence of climatic variations? Palaeogeogr. Palaeoclimatol. Palaeoecol. 369, 163–174. https://doi.org/10.1016/j.palaeo.2012.10.016.

Faivre, S., Bakran-Petricioli, T., Barešić, J., Horvatinčić, N., 2015. New data on the marine radiocarbon reservoir effect in the Eastern Adriatic based on pre-bomb marine organisms from the intertidal zone and shallow sea. Radiocarbon 57 (4), 527–538. https://doi.org/10.2458/azu_rc.57.18452.

Faivre, S., Bakran-Petricioli, T., Barešić, J., Horvatić, D., Macario, K., 2019a. Relative Sea-level change and climate change in the Northeastern Adriatic during last 1.5 ka (Istria, Croatia). Quat. Sci. Rev. 222, 105909. https://doi.org/10.1016/j.quascirev.2019.105909.

Faivre, S., Bakran-Petricioli, T., Barešić, J., Morhange, C., Borković, D., 2019b. Marine radiocarbon reservoir age of the coralline intertidal alga *Lithophyllum byssoides* in the Mediterranean. Quat. Geochronol. 51, 15–23. https://doi.org/10.1016/j.quageo.2018.12.002.

Faivre, S., Bakran-Petricioli, T., Barešić, J., Horvatić, D., 2021a. *Lithophyllum* rims as biological markers for constraining palaeoseismic events and relative sea-level variations during the last 3.3 ka on Lopud Island, southern Adriatic, Croatia. Glob. Planet. Chang. 202, 103517. https://doi.org/10.1016/j.gloplacha.2021.103517.

Faivre, S., Bakran-Petricioli, T., Herak, M., Barešić, J., Borković, D., 2021b. Late Holocene interplay between coseismic uplift events and interseismic subsidence at Koločep island and Grebeni islets in the Dubrovnik archipelago (southern Adriatic, Croatia). Quat. Sci. Rev. 274, 107284. https://doi.org/10.1016/j.quascirev.2021.107284.

Ferranti, L., Antonioli, F., Mauz, B., Amorosi, A., Dai Pra, G., Mastronuzzi, G., Monaco, C., Orrù, P., Pappalardo, M., Radtke, U., Renda, P., Romano, P., Sansò, P., Verrubbi, V., 2006. Markers of the last interglacial sea-level high stand along the coast of Italy: tectonic implications. Quat. Int. 145–146, 30–54. https://doi.org/10.1016/j.quaint.2005.07.009.

Fouache, E., Faivre, S., Dufaure, J.-J., Kovačić, V., Tassaux, F., 2000. New observations on the evolution of the Croatian shoreline between Poreč and Zadar over the past 2000 years, Zeitschrift für Geomorphologie N.F. Supplementband S122, 33–46.

Gačić, M., Eusebi Borzelli, G.L., Civitarese, G., Cardin, V., Yari, S., 2010. Can internal processes sustain reversals of the ocean upper circulation? The Ionian Sea example. Geophys. Res. Lett. 37 (9), L09608. https://doi.org/10.1029/2010GL043216.

Gačić, M., Civitarese, G., Eusebi Borzelli, G.L., Kovačević, V., Poulain, P.-M., Theocharis, A., Menna, M., Catucci, A., Zarokanellos, N., 2011. On the relationship between the decadal oscillations of the Northern Ionian Sea and the salinity distributions in the Eastern Mediterranean. J. Geophys. Res. 116, C12002. https://doi.org/10.1029/2011JC007280.

Gehrels, W.R., Kirby, J.R., Prokoph, A., Newnham, R.M., Achterberg, E.P., Evans, H., Black, S., Scott, D.B., 2005. Onset of recent rapid sea-level rise in the western Atlantic Ocean. Quat. Sci. Rev. 24 (18–19), 2083–2100. https://doi.org/10.1016/j.quascirev.2004.11.016.

Govorčin, M., Herak, M., Matoš, B., Pribičević, B., Vlahović, I., 2020. Constraints on complex Faulting during the 1996 Ston-Slano (Croatia) Earthquake Inferred from the DInSAR. Seismol. Geol. Observat. Remote Sens. 12 (7), 1157. https://doi.org/10.3390/rs12071157.

Gregory, J.M., Griffies, S.M., Hughes, C.W., Lowe, J.A., Church, J.A., Fukimori, I., Gomez, N., Kopp, R.E., Landerer, F., Le Cozannet, G., Ponte, R.M., Stammer, D., Tamisiea, M.E., van de Wal, R.S.W., 2019. Concepts and Terminology for Sea Level: mean, Variability and Change, both local and Global. Surv. Geophys. 40, 1251–1289. https://doi.org/10.1007/s10712-019-09525-z.

Grenerczy, G., Sella, G., Stein, S., Kenyeres, A., 2005. Tectonic implications of the GPS velocity field in the northern Adriatic region. Geophys. Res. Lett. 32, L16311. https://doi.org/10.1029/2005GL022947.

Heaton, T.J., Köhler, P., Butzin, M., Bard, E., Reimer, R.W., Austin, Wen, Bronk Ramsey, C., Hughen, K.A., Kromer, B., Reimer, P.J., Adkins, J., Burke, A., Cook, M.S., Olsen, J., Skinner, L.C., 2020. Marine20 - the marine radiocarbon age calibration curve (0-55, 000 cal BP). Radiocarbon 62 (4), 779–820. https://doi.org/10.1017/RDC.2020.68.

Herak, M., Herak, D., Markušić, S., 1996. Revision of the earthquake catalogue and seismicity of Croatia, 1908-1992. Terra Nova 8 (1), 86–94. https://doi.org/10.1111/j.1365-3121.1996.tb00728.x.

Ilijanić, N., Miko, S., Ivkić Filipović, I., Hasan, O., Šparica Miko, M., Petrinec, B., Terzić, J., Marković, T., 2022. A Holocene Sedimentary Record and the Impact of Sea-Level rise in the Karst Lake Velo Blato and the Wetlands on Pag Island (Croatia). Water 14, 342. https://doi.org/10.3390/w14030342.

Incarbona, A., Martrat, B., Mortyn, P.G., Sprovieri, M., Ziveri, P., Gogou, A., Jordà, G., Xoplaki, E., Luterbacher, J., Langone, L., Marino, G., Rodríguez-Sanz, L., Triantaphyllou, M., Di Stefano, E., Grimalt, J.O., Tranchida, G., Sprovieri, R., Mazzola, S., 2016. Mediterranean circulation perturbations over the last five centuries: Relevance to past Eastern Mediterranean Transient-type events. Sci. Rep. 6, 29623. https://doi.org/10.1038/srep29623.

Kaniewski, D., Marriner, N., Morhange, C., Rius, D., Carre, M.-B., Faivre, S., Van Campo, E., 2018. Croatia's mid-late Holocene (5200-3200 BP) coastal vegetation shaped by human societies. Quat. Sci. Rev. 200, 334–350. https://doi.org/10.1016/j.quascirev.2018.10.004.

Kaniewski, D., Marriner, N., Cheddadi, R., Morhange, C., Vacchi, M., Rovere, A., Faivre, S., Otto, T., Lucek, F., Carre, M.-B., Benčić, G., Van Campo, E., 2021. Coastal submersions in the north-eastern Adriatic during the last 5200 years. Glob. Planet. Chang. 204, 103570. https://doi.org/10.1016/j.gloplacha.2021.103570.

Kaniewski, D., Marriner, N., Sarti, G., Bertoni, D., Marchesini, M., Rossi, V., Lena, A., Bivolaru, A., Pourkerman, M., Vacchi, M., Cheddadi, R., Otto, T., Luce, F., Cottica, D., Morhange, C., 2022. Northern Adriatic environmental changes since 500 AD reconstructed at Aquileia (Italy). Quat. Sci. Rev. 287, 107565. https://doi.org/10.1016/j.quascirev.2022.107565.

Kastelic, V., Carafa, M.M.C., 2012. Fault slip rates for the active External Dinarides thrust-and-fold belt. Tectonics 31. https://doi.org/10.1029/2011TC003022. . s.

Kastelic, V., Vannoli, P., Burrato, P., Fracassi, U., Tiberti, M.M., Valensise, G., 2013. Seismogenic sources in the Adriatic Domain. Mar. Pet. Geol. 42, 191–213. https://doi.org/10.1016/j.marpetgeo.2012.08.002.

Kemp, A.C., Hawkes, A.D., Donnelly, J.P., Vane, C.H., Horton, B.P., Hill, T.D., Anisfeld, S.C., Parnell, A.C., Cahill, N., 2015. Relative Sea-level change in Connecticut (USA) during the last 2200 yrs. Earth Planet. Sci. Lett. 428, 217–229. https://doi.org/10.1016/j.epsl.2015.07.034.

Kemp, A.C., Wright, A.J., Edwards, R.J., Barnett, R.L., Brain, M.J., Kopp, R.E., Cahill, N., Horton, B.P., Charman, D.J., Hawkes, A.D., Hill, T.D., van de Plassche, O., 2018. Relative Sea-level change in Newfoundland, Canada during the past 3000 years. Quat. Sci. Rev. 201, 89–110. https://doi.org/10.1016/j.quascirev.2018.10.012.

Kench, P.S., McLean, R.F., Owen, S.D., Ryan, E., Morgan, K.E., Ke, L., Wang, X., Roy, K., 2020. Climate-forced Sea-level lowstands in the Indian Ocean during the last two millennia. Nat. Geosci. 13, 61–64. https://doi.org/10.1038/s41561-019-0503-7.

Khan, N.S., Horton, B., Engelhart, S., Rovere, A., Vacchi, M., Ashe, E.L., Törnqvist, T.E., Dutton, A., Hijma, M.P., Shennan, I., 2019. Inception of a global atlas of sea levels since the last Glacial Maximum. Quat. Sci. Rev. 220, 359–371. https://doi.org/10.1016/j.quascirev.2019.07.016.

Kišpatić, M., 1891. Earthquakes in Croatia (in Croatian). Rad Jugoslavenske Akademije Znanosti i Umjetnosti (Paper of Yugoslav Academy of Science and Art Zagreb). 107. pp. 81–164.

Kopp, R.E., Kemp, A.C., Bittermann, K., Horton, B.P., Donnelly, J.P., Gehrels, W.R., Hay, C.C., Mitrovica, J.X., Morrow, E.D., Rahmstorf, S., 2016. Temperature-driven global sea-level variability in the Common Era. Proceed. Nat. Acad. Sci. USA 113, E1434–E1441. https://doi.org/10.1073/pnas.1517056113.

Korbar, T., Montanari, A., Koch, G., Mariani, S., DePaolo, D., Turchyn, A., Miknić, M., Tari, V., 2009. Geologic reconnaissance of the island of Velika Palagruža (central Adriatic, Croatia). Geol. Croatic. 62 (2), 75–94. https://doi.org/10.4154/GC.2009.07.

Kovačić, M., Pavelić, D., Vlahović, I., Marković, F., Wacha, L., Kampić, Š., Rončević, S., Drempetić, D., 2018. Pleistocene alluvial and aeolian deposits with tephra on the island of Lopud (eastern mid- Adriatic, Croatia): provenance, wind regime, and climate controls. Quat. Int. 494, 92–104. https://doi.org/10.1016/j.quaint.2017.11.054.

Krajcar Bronić, I., Horvatinčić, N., Sironić, A., Obelić, B., Barešić, J., Felja, I., 2010. A new graphite preparation line for AMS ^{14}C dating in the Zagreb Radiocarbon Laboratory. Nucl. Inst. Methods Phys. Res. B 268 (7–8), 943–946. https://doi.org/10.1016/j.nimb.2009.10.070.

Kuk, V., Prelogović, E., Dragičević, I., 2000. Seismotectonically active zones in the Dinarides. Geol. Croatic. 53 (2), 295–303. https://doi.org/10.4154/GC.2000.06.

Laborel, J., 1979. Fixed marine organisms as biological indicators for the study of recent sea level and climatic variations along the Brazilian tropical coast. In: Proceedings of 1978 International Symposium on Coastal Evolution in the Quaternary. São Paulo. pp. 193–211.

Laborel, J., 1987. Marine biogenic constructions in the Mediterranean. In: Scientific Reports of the Port-Cros National Park, 13, pp. 97–126.

Laborel, J., Laborel-Deguen, F., 1994. Biological indicators of relative sea-level variations and of co-seismic displacements in the Mediterranean region. J. Coast. Res. 10 (2), 395–415.

Laborel, J., Delibrias, G., Boudouresque, C.F., 1983. Variations récentes du niveau marin à Port-Cros (Var, France), mises en évidence par l'étude de la corniche littorale à *Lithophyllum tortuosum*. In: Comptes Rendus de l'Académie des Sciences, France, 297 Séries II. pp. 157–160.

Laborel, J., Morhange, C., Lafont, R., Le Campion, J., Laborel-Deguen, F., Sartoretto, S., 1994. Biological evidence of sea-level rise during the last 4500 years on the rocky coasts of continental southwestern France and Corsica. Mar. Geol. 120, 203–223. https://doi.org/10.1016/0025-3227(94)90059-0.

Lambeck, K., Antonioli, F., Anzidei, M., Ferranti, L., Leoni, G., Scicchitano, G., Silenzi, S., 2011. Sea level change along the Italian coast during the Holocene and projections for the future. Quat. Int. 232 (1–2), 250–257. https://doi.org/10.1016/j.quaint.2010.04.026.

Lambeck, K., Rouby, H., Purcell, A., Sun, Y., Sambridge, M., 2014. Sea level and global ice volumes from the last Glacial Maximum to the Holocene. In: Proceedings of the National Academy of Sciences USA, 111, pp. 15296–15303. https://doi.org/10.1073/pnas.1411762111.

Leng, M.J., Marshall, J.D., 2004. Palaeoclimate interpretation of stable isotope data from lake sediments. Quat. Sci. Rev. 23, 811–831. https://doi.org/10.1016/j.quascirev.2003.06.012.

Ljungqvist, F.C., 2010. A new reconstruction of temperature variability in the extratropical Northern Hemisphere during the last two millennia. Geogr. Ann. 92A (3), 339–351. https://doi.org/10.1111/j.1468-0459.2010.00399.x.

Lončar, N., Bar-Matthews, M., Ayalon, A., Surić, M., Faivre, S., 2017. Early and Mid-Holocene environmental conditions in the Eastern Adriatic recorded in speleothems from Mala špilja Cave and Velika špilja Cave (Mljet Island, Croatia). Acta Carsolog. 46 (2–3), 229–249. https://doi.org/10.3986/ac.v46i2-3.4939.

Lončar, N., Bar-Matthews, M., Ayalon, A., Faivre, S., Surić, M., 2019. Holocene climatic conditions in the Eastern Adriatic recorded in stalagmites from Strašna peć Cave (Croatia). Quat. Int. 508, 98–106. https://doi.org/10.1016/j.quaint.2018.11.006.

Lončar, N., Surić, M., Bar-Matthews, M., Faivre, S., Ayalon, A., 2022. Climate variability in southern Croatia from the end of MIS 5 through the last glacial period recorded in speleothems from Mljet island caves. Zeitschrift für Geomorphol. N.F. 63 (2–3), 245–263. https://doi.org/10.1127/zfg/2022/0739.

Manca, B.B., Kovačević, V., Gačić, M., Viezzoli, D., 2002. Dense water formation in the Southern Adriatic Sea and spreading into the Ionian Sea in the period 1997-1999. J. Mar. Syst. 33–34, 133–154. https://doi.org/10.1016/S0924-7963(02)00056-8.

Mann, M.E., Zhang, Z., Hughes, M.K., Bradley, R.S., Miller, S.K., Rutherford, S., Ni, F., 2008. Proxy-based reconstructions of hemispheric and global surface temperature variations over the past two millennia. Proceed. Nat. Acad. Sci. USA 105 (36), 13252–13257. https://doi.org/10.1073/pnas.0805721105.

Marković, B., 1971. Basic Geological Map of SFRY, M 1:100.000, Dubrovnik Sheet K34-49. Federal Geological Institute, Beograd, Serbia.

Marriner, N., Morhange, C., Faivre, S., Flaux, C., Vacchi, M., Miko, S., Boetto, G., Radić Rossi, I., 2014. Post-Roman Sea-level changes on Pag Island (Adriatic Sea): dating Croatia's "enigmatic" coastal notch? Geomorphology 221, 83–94. https://doi.org/10.1016/j.geomorph.2014.06.002.

Marriner, N., Kaniewski, D., Pourkerman, M., Devillers, B., 2022. Anthropocene tipping point reverses long-term Holocene cooling of the Mediterranean Sea: a meta-analysis of the basin's Sea Surface Temperature records. Earth Sci. Rev. 227, 103986. https://doi.org/10.1016/j.earscirev.2022.103986.

Mihanović, H., Vilibić, I., Dunić, N., Šepić, J., 2015. Mapping of decadal middle Adriatic oceanographic variability and its relation to the BiOS regime. J. Geophys. Res. Oceans 120 (8), 5615–5630. https://doi.org/10.1002/2015JC010725.

Moberg, A., Sonechkin, D.M., Holmgren, K., Datsenko, N.M., Karlén, W., 2005. Highly variable Northern Hemisphere temperatures reconstructed from low- and high-resolution proxy data. Nature 433, 613–617. https://doi.org/10.1038/nature03265.

Morhange, C., 1994. La mobilité récente des littoraux provençaux (The recent mobility of the Provencal littoral). Thèse de doctorat en Géographie Physique. Université de Provence, Centre d'Aix, Faculté des Lettres et des Sciences Humaines. Institut de Geography.

Morhange, C., Marriner, N., 2015. Archaeological and biological relative sea-level indicators, chapter 9. In: Shennan, I., Long, A.J., Horton, B.P. (Eds.), Handbook of Sea Level Research. Wiley, pp. 146–156. https://doi.org/10.1002/9781118452547.ch9.

Morhange, C., Laborel, J., Hesnard, A., 2001. Changes of relative sea level during the past 5000 years in the ancient harbor of Marseilles, Southern France. Palaeogeogr. Palaeoclimatol. Palaeoecol. 166 (3–4), 319–329. https://doi.org/10.1016/S0031-0182(00)00215-7.

Natević, L.J., Petrović, V., 1967. Basic Geological Map of the SFRY, M 1:100.000, Trebinje Sheet K34-37. Federal Geological Institute, Beograd, Serbia.

Neukom, R., Barboza, L.A., Erb, M.P., Shi, F., Geay, J.E., Evans, M.N., Franke, J.,

Kaufman, D.S., Lücke, L., Rehfeld, K., Schurer, A., Zhu, F., Brönnimann, S., Hakim, G.J., Henley, B.J., Ljungqvist, F.C., McKay, N., Valler, V., von Gunten, L., PAGES 2k Consortium, 2019. Consistent multidecadal variability in global temperature reconstructions and simulations over the Common Era. Nat. Geosci. 12, 643–649. https://doi.org/10.1038/s41561-019-0400-0.

Onac, B.P., Mitrovica, J.X., Ginés, J., Asmerom, Y., Polyak, V.J., Tuccimei, P., Ashe, E.L., Fornós, J.J., Hoggard, M.J., Coulson, S., Ginés, A., Soligo, M., Villa, I.M., 2022. Exceptionally stable preindustrial sea level inferred from the western Mediterranean Sea. Sci. Adv. 8 (26), eabm6185. https://doi.org/10.1126/sciadv.abm6185.

PAGES 2k Consortium, 2013. Continental-scale temperature variability during the past two millennia. Nat. Geosci. 6, 339–346. https://doi.org/10.1038/ngeo1797.

Palenik, D., Matičec, D., Fuček, D., Matoš, B., Herak, M., Vlahović, I., 2019. Geological and structural setting of the Vinodol Valley (NW Adriatic, Croatia): insights into its tectonic evolution based on structural investigations. Geol. Croatic. 72 (3), 179–193. https://doi.org/10.4154/gc.2019.13.

Peltier, W.R., 1996. Global sea level rise and glacial isostatic adjustment: an analysis of data from the east coast of North America. Geophys. Res. Lett. 23 (7), 717–720. https://doi.org/10.1029/96GL00848.

Pérès, J.M., Picard, J., 1964. Nouveau manuel de bionomie benthique en Méditerranée. Recueil des travaux de la Station marine d'Endoume 31 (47), 1–131.

Prelogović, E., Pribičević, B., Ivković, Ž., Dragićević, I., Buljan, R., Tomljenović, B., 2004. Recent structural fabric of the Dinarides and tectonically active zones important for petroleum-geological exploration. Nafta: Explorat., Product., Process., Petrochem. 55 (4), 155–161.

Prtoljan, B., Jamičić, D., Cvetko Tešović, B., Kratković, I., Markulin, Ž., 2007. The influence of late cretaceous synsedimentary deformation on the Cenozoic structuration of the middle Adriatic, Croatia. Geodin. Acta 20 (5), 287–300. https://doi.org/10.3166/ga.20.287-300.

Raić, V., Papeš, J., Ahac, A., Korolija, B., Borović, I., Grimani, I., Marinčić, S., 1980. Basic Geological Map of SFRY, M 1:100.000, Ston Sheet K33-48. Federal Geological Institute, Beograd, Serbia.

Razum, I., Miko, S., Ilijanić, N., Petrelli, M., Röhl, U., Hasan, O., Giaccio, B., 2020. Holocene tephra record of lake Veliko jezero, Croatia: implications for the Central Mediterranean tephrostratigraphy and sea level rise. Boreas 49 (3), 653–673. https://doi.org/10.1111/bor.12446.

Révész, K.M., Landwehr, J.M., 2002. $\delta^{13}C$ and $\delta^{18}O$ isotopic composition of $CaCO_3$ measured by continuous flow isotope ratio mass spectrometry: statistical evaluation and verification by application to Devils Hole core DH-11 calcite. Rapid Commun. Mass Spectrom. 16, 2102–2114. https://doi.org/10.1002/rcm.833.

Rietbroek, R., Brunnabend, S.-E., Kusche, J., Schröter, J., Dahle, C., 2016. Revisiting the contemporary sea-level budget on global and regional scales. Proceed. Nat. Acad. Sci. USA 113 (6), 1504–1509. https://doi.org/10.1073/pnas.1519132113.

Roemmich, D., Gilson, J., 2009. The 2004-2008 mean and annual cycle of temperature, salinity, and steric height in the global ocean from the Argo Program. Prog. Oceanogr. 82, 81–100. https://doi.org/10.1016/j.pocean.2009.03.004.

Roether, W., Klein, B., Manca, B.B., Theocharis, A., Kioroglou, S., 2007. Transient Eastern Mediterranean deep waters in response to the massive dense-water output of the Aegean Sea in the 1990s. Prog. Oceanogr. 74 (4), 540–571. https://doi.org/10.1016/j.pocean.2007.03.001.

Rovere, A., Stocchi, P., Vacchi, M., 2016. Eustatic and Relative Sea Level changes. Curr. Climate Change Reports 2, 221–231. https://doi.org/10.1007/s40641-016-0045-7.

Rudzka, D., McDermott, F., Surić, M., 2012. A late Holocene climate record in stalagmites from Modrič Cave (Croatia). J. Quat. Sci. 27 (6), 585–596. https://doi.org/10.1002/jqs.2550.

Schembri, P.J., Deidun, A., Mallia, A., Mercieca, L., 2005. Rocky shore biotic assemblages of the Maltese Islands (Central Mediterranean): a conservation perspective. J. Coast. Res. 21 (1), 157–166.

Schmid, S.M., Fügenschuh, B., Kounov, A., Maţenco, L., Nievergelt, P., Oberhänsli, R., Pleuger, J., Schefer, S., Schuster, R., Tomljenović, B., Ustaszewski, K., van Hinsbergen, D.J., 2020. Tectonic units of the Alpine collision zone between Eastern Alps and Western Turkey. Gondwana Res. 78, 308–374. https://doi.org/10.1016/j.gr.2019.07.005.

Schmitz, B., Biermanns, P., Hinsch, R., Đaković, M., Onuzi, K., Reicherter, K., Ustaszewski, K., 2020. Ongoing shortening in the Dinarides fold-and-thrust belt: a new structural model of the 1979 (Mw 7.1) Montenegro earthquake epicentral region. J. Struct. Geol. 141, 104192. https://doi.org/10.1016/j.jsg.2020.104192.

Sechi, D., Andreucci, S., Pascucci, V., 2018. Intertidal Upper Pleistocene algal build-ups (Trottoir) of NW Sardinia (Italy): a tool for past sea level reconstruction. J. Mediterranean Earth Sci. 10, 167–171. https://doi.org/10.3304/JMES.2018.009.

Sechi, D., Andreucci, S., Stevens, T., Pascucci, V., 2020. Age and significance of late Pleistocene *Lithophyllum byssoides* intertidal algal ridge, NW Sardinia, Italy. Sediment. Geol. 400, 105618. https://doi.org/10.1016/j.sedgeo.2020.105618.

Shaw, T.A., Plater, A.J., Kirby, J.R., Roy, K., Holgate, S., Tutman, P., Cahill, N., Horton, B.P., 2018. Tectonic influences on late Holocene relative sea levels from the central-eastern Adriatic coast of Croatia. Quat. Sci. Rev. 200, 262–275. https://doi.org/10.1016/j.quascirev.2018.09.015.

Shennan, I., 2015. Handbook of sea-level research: Framing research questions. Oxford. In: Shennan, I., Long, A.J., Horton, B.P. (Eds.), Handbook of Sea-Level Research. John Wiley & Sons, pp. 3–25.

Shindell, D.T., Schmidt, G.A., Mann, M.E., Rind, D., Waple, A., 2001. Solar forcing of regional climate change during the Maunder Minimum. Science 294, 2149–2152. https://doi.org/10.1126/science.1064363.

Siani, G., Magny, M., Paterne, M., Debret, M., Fontugne, M., 2013. Paleohydrology reconstruction and Holocene climate variability in the South Adriatic Sea. Clim. Past 9, 499–515. https://doi.org/10.5194/cp-9-499-2013.

Silenzi, S., Antonioli, F., Chemello, R., 2004. A new marker for sea surface temperature trend during the last centuries in temperate areas: vermetid reef. Glob. Planet. Chang. 40, 105–114. https://doi.org/10.1016/S0921-8181(03)00101-2.

Sisma-Ventura, G., Guzner, B., Yam, R., Fine, M., Shemesh, A., 2009. The reef builder gastropod *Dendropoma petraeum* - a proxy of short and long term climatic events in the Eastern Mediterranean. Geochim. Cosmochim. Acta 73 (15), 4376–4383. https://doi.org/10.1016/j.gca.2009.04.037.

Šolaja, D., Miko, S., Brunović, D., Ilijanić, N., Hasan, O., Papatheodorou, G., Geraga, M., Durn, T., Christodoulou, D., Razum, I., 2022. Late Quaternary Evolution of a Submerged Karst Basin Influenced by active Tectonics (Koločep Bay, Croatia). J. Marine Sci. Eng. 10, 881. https://doi.org/10.3390/jmse10070881.

Spampinato, C.R., Ferranti, L., Monaco, C., Scicchitano, G., Antonioli, F., 2014. Raised Holocene paleo-shorelines along the Capo Vaticano coast (western Calabria, Italy): evidence of co-seismic and steady-state deformation. J. Geodyn. 82, 178–193. https://doi.org/10.1016/j.jog.2014.03.003.

Spötl, C., Vennemann, T.W., 2003. Continuous-flow isotope ratio mass spectrometric analysis of carbonate minerals. Rapid Commun. Mass Spectrom. 17, 1004–1006. https://doi.org/10.1002/rcm.1010.

Stammer, D., Cazenave, A., Ponte, R.M., Tamisiea, M.E., 2013. Causes for contemporary regional sea level changes. Annu. Rev. Mar. Sci. 5, 21–46. https://doi.org/10.1146/annurev-marine-121211-172406.

Steinhilber, F., Beer, J., Frölich, C., 2009. Total solar irradiance during the Holocene. Geophys. Res. Lett. 36, L19704. https://doi.org/10.1029/2009GL040142.

Stewart, I.S., Morhange, C., 2009. Coastal geomorphology and sea-level change. In: Woodward, J.C. (Ed.), The Physical Geography of the Mediterranean. Oxford University Press, Oxford, pp. 385–413.

Stiros, S.C., Pirazzoli, P.A., 2008. Direct determination of tidal levels for engineering applications based on biological observations. Coast. Eng. 55 (6), 459–467. https://doi.org/10.1016/j.coastaleng.2008.01.005.

Stocchi, P., Spada, G., 2009. Influence of glacial isostatic adjustment upon current sea level variations in the Mediterranean. Tectonophysics 474, 56–68. https://doi.org/10.1016/j.tecto.2009.01.003.

Stuiver, M., Polach, H.A., 1977. Discussion: reporting of ^{14}C data. Radiocarbon 19 (3), 355–363. https://doi.org/10.1017/S0033822200003672.

Surić, M., 2018. Speleothem-based Quaternary research in Croatian karst – a review. Quat. Int. 490, 113–122. https://doi.org/10.1016/j.quaint.2018.04.043.

Surić, M., Korbar, T., Juračić, M., 2014. Tectonic constraints on the late Pleistocene-Holocene relative sea-level change along the north-eastern Adriatic coast (Croatia). Geomorphology 220, 93–103. https://doi.org/10.1016/j.geomorph.2014.06.001.

Talbot, M.R., 1990. A review of the paleohydrological interpretation of carbon and oxygen isotopic rations in primary lacustrine carbonates. Chem. Geol.: Isotope Geosci. Sect. 80 (4), 261–279. https://doi.org/10.1016/0168-9622(90)90009-2.

Topić, N., Bedić, Ž., Vyroubal, V., Šlaus, M., Barešić, J., Sironić, A., Ilkić, M., Moore, A.M.T., Drašković Vlašić, N., 2019. Inventar nalaza i višefazno groblje uz utvrdu Sokol u Konavlima (Inventory of finds and multiphase cemetery by Fort Sokol in Konavle). Archaeolog. Adriatic. 13, 107–251. (in Croatian and English). 10.15291/archeo.3302.

Tzedakis, P.C., Drysdale, R., Margari, V., Skinner, L.C., Menviel, L., Parrenin, F., Taschetto, A.S., Hellstrom, J.C., Regattieri, E., Zanchetta, G., Fallick, A.E., Crowhurst, S.J., Martrat, B., Grimalt, J.O., Roe, K., Mokeddem, Z., Mcmanus, J.F., Hodell, D.A., 2018. Enhanced climate instability in the North Atlantic and Europe during the last Interglacial. Nat. Commun. https://doi.org/10.1038/s41467-018-06683-3.

Usoskin, I.G., Arlt, R., Asvestari, E., Hawkins, E., Käpylä, M., Kovaltsov, G.A., Krivova, N., Lockwood, M., Mursula, K., O'Reilly, J., Owens, M., Scott, C.J., Sokoloff, D.D., Solanki, S.K., Soon, W., Vaquero, J.M., 2015. The Maunder minimum (1645-1715) was indeed a grand minimum: a reassessment of multiple datasets. Astron. Astrophys. 581, A95. https://doi.org/10.1051/0004-6361/201526652.

Ustaszewski, K., Kounov, A., Schmid, S.M., Schaltegger, U., Krenn, E., Frank, W., Fügenschuh, B., 2010. Evolution of the Adria–Europe plate boundary in the northern Dinarides: from continent–continent collision to back-arc extension. Tectonics 29, TC6017. https://doi.org/10.1029/2010TC002668.

Vacchi, M., Marriner, N., Morhange, C., Spada, G., Fontana, A., Rovere, A., 2016. Multiproxy assessment of Holocene relative sea-level changes in the western Mediterranean: sea-level variability and improvements in the definition of the isostatic signal. Earth Sci. Rev. 155, 172–197. https://doi.org/10.1016/j.earscirev.2016.02.002.

van Hinsbergen, D.J.J., Torsvik, T.H., Schmid, S.M., Maţenco, L.C., Maffione, M., Vissers, R.L.M., Gürer, D., Spakman, W., 2020. Orogenic architecture of the Mediterranean region and kinematic reconstruction of its tectonic evolution since the Triassic. Gondwana Res. 81, 79–229. https://doi.org/10.1016/j.gr.2019.07.009.

van Unen, M., Matenco, L., Nader, F.H., Darnault, R., Mandic, O., Demir, V., 2019a. Kinematics of Foreland-Vergent Crustal Accretion: Inferences from the Dinarides Evolution. Tectonics 38, 49–76. https://doi.org/10.1029/2018TC005066.

van Unen, M., Matenco, L., Demir, V., Nader, F.H., Darnault, R., Mandic, O., 2019b. Transfer of deformation during indentation: Inferences from the post-middle Miocene evolution of the Dinarides. Glob. Planet. Chang. 182, 103027. https://doi.org/10.1016/j.gloplacha.2019.103027.

Vlahović, I., Tišljar, J., Velić, I., Matičec, D., 2005. Evolution of the Adriatic Carbonate Platform: Palaeogeography, main events and depositional dynamics. Palaeogeogr. Palaeoclimatol. Palaeoecol. 220, 333–360. https://doi.org/10.1016/j.palaeo.2005.01.011.

Vlahović, I., Mandic, O., Mrinjek, E., Bergant, S., Ćosović, V., de Leeuw, A., Enos, P., Hrvatović, H., Matičec, D., Mikša, G., Nemec, W., Pavelić, D., Pencinger, V., Velić, I., Vranjković, A., 2012. Marine to continental depositional systems of Outer Dinarides foreland and intra-montane basins (Eocene-Miocene, Croatia and Bosnia and Herzegovina). J. Alpine Geol. 54, 405–470.

Walker, J.S., Kopp, R.E., Shaw, T.A., Cahill, N., Khan, N.S., Barber, D.C., Ashe, E.L., Brain,

M.J., Clear, J.L., Corbett, D.R., Horton, B.P., 2021. Common Era Sea-level budgets along the U.S. Atlantic coast. Nat. Commun. 12, 1841. https://doi.org/10.1038/s41467-021-22079-2.

Weber, J., Vrabec, M., Pavlovčič-Prešeren, P., Dixon, T., Jiang, Y., Stopar, B., 2010. GPS-derived motion of the Adriatic microplate from Istria Peninsula and Po Plain sites, and geodynamic implications. Tectonophysics 483, 214–222. https://doi.org/10.1016/j.tecto.2009.09.001.

Williams, C.K.I., Rasmussen, C.E., 1996. Gaussian Processes for Regression. MIT Press, Cambridge.

Yiou, P., Servonnat, J., Yoshimori, M., Swingedouw, D., Khodri, M., Abe-Ouchi, A., 2012. Stability of weather regimes during the last millennium from climate simulations. Geophys. Res. Lett. 39, L08703. https://doi.org/10.1029/2012GL051310.